Street-level methane emissions of Bucharest, Romania and the dominance of urban wastewater.

J.M. Fernandez [a,*], H. Maazallahi [b,c], J.L. France [a,e], M. Menoud [b], M. Corbu [d], M. Ardelean [d], A. Calcan [d], A. Townsend-Small [f], C. van der Veen [b], R.E. Fisher [a], D. Lowry [a], E.G. Nisbet [a], T. Röckmann [b]

[a] Department of Earth Sciences, Royal Holloway University of London, Egham, TW20 0EX, United Kingdom
[b] Institute for Marine and Atmospheric Research Utrecht, Utrecht University, Utrecht, the Netherlands
[c] Netherlands Organization for Applied Scientific Research (TNO), Utrecht, the Netherlands
[d] National Institute of Aerospace Research "ELIE CAROFOLI" - INCAS, Bucharest, 061126, Romania
[e] British Antarctic Survey, Natural Environment Research Council, Cambridge, CB3 0ET, United Kingdom
[f] Department of Geology, University of Cincinnati, Cincinnati, OH, 45221, USA

ARTICLE INFO

ABSTRACT

Atmospheric methane (CH_4) continues to increase, but there are multiple anthropogenic source categories that can be targeted for cost-effective emissions reduction. Cities emit CH_4 to the atmosphere from a mixture of anthropogenic CH_4 sources, which include, but are not limited to, fugitive emissions from natural gas distribution systems, wastewater treatment facilities, waste-and rainwater networks, and landfills. Therefore, to target mitigation measures, it is important to locate and quantify local urban emissions to prioritize mitigation opportunities in large cities. Using mobile measurement techniques, we located street-level CH_4 leak indications, measured flux rates, and determined potential source origins (using carbon and hydrogen stable isotopic composition along with ethane: CH_4 ratios) of CH_4 in Bucharest, Romania. We found 969 confirmed CH_4 leak indication locations, where the maximum mole fraction elevation (above background) was 38.3 ppm (mean = 0.9 ppm $\pm$ 0.1 ppm s.e.; n = 2482). Individual leak indicator fluxes, derived using a previously established empirical relation, ranged up to around 15 metric tons CH_4 yr^{-1} (mean = 0.8 metric tons yr^{-1} $\pm$ 0.05, s.e.; n = 969). The total estimated city emission rate is 1832 tons CH_4 yr^{-1} (min = 1577 t yr^{-1} and max = 2113 t yr^{-1}). More than half (58%–63%) of the CH_4 elevations were attributed to biogenic wastewater, mostly from venting storm grates and manholes connecting to sewer pipelines. Hydrogen isotopic composition of CH_4 and ethane:methane ratios were the most useful tracers of CH_4 sources, due to similarities in carbon isotope ratios between wastewater gas and natural gas. The annual city-wide CH_4 emission estimate of Bucharest exceeded emissions of Hamburg, Germany by 76% and Paris, France by 90%.

1. Introduction

Methane (CH_4) is a major greenhouse gas (GHG), with a global warming potential 28 times that of CO_2 over 100 years (IPCC AR5, Myhre et al., 2013). Methane's shorter atmospheric lifetime compared to CO_2 of around a decade makes it an attractive target for rapid GHG reduction efforts. The atmospheric CH_4 burden has more than doubled over the past 200 years (Mischler et al., 2009; Saunois et al., 2020; Sowers et al., 2010), reaching a global annual average of 1877 $\pm$ 2 ppb in 2019 (WMO, 2020). Although we have a good qualitative understanding on various naturally produced (wetlands, freshwater, geological activity, etc.) and anthropogenically induced CH_4 sources (fossil fuel production, agricultural practices, waste management, etc.) (Kirschke et al., 2013), there still remain discrepancies on how these sources contribute to CH_4 budgets and isotopic balance locally and regionally (Miller et al., 2013; Saunois et al., 2020; Sherwood et al., 2017; Worden et al., 2017; Zazzeri et al., 2017). It is important to understand and discriminate between these source inputs at regional and local scales in order to identify mitigation opportunities, in order to halt the presently

Abbreviations

CH_4	Methane
C_2H_6	Ethane
C_2:	C_1 - Ethane:methane ratio
CO_2	Carbon dioxide
CRDS	Cavity ringdown spectroscopy
GHG	Greenhouse gas
IRMS	Isotope ratio mass spectrometry
LI	Leak indicator
LGRUMEA	Los Gatos Research Ultraportable Methane/Ethane Analyzer
MPI	Max Plank Institute
NOAA	National Oceanic and Atmospheric Administration
RHUL	Royal Holloway, University of London
s.d.	Standard deviation (1st)
s.e.	Standard error
UU	Utrecht University
WMO	World Meterological Organization

ongoing rapid global CH_4 increases (Dlugokencky et al., 2011; Nisbet et al., 2019) and bring the global CH_4 burden back to a pathway required to comply with the United Nations (UN) Paris Agreement (Nisbet et al., 2020).

Over the past decade, there has been a growing research interest in identifying and quantifying fugitive CH_4 emissions from populated regions, specifically in urbanized areas. Studies of U.S. cities like Los Angeles, California and Boston, Massachusetts have shown that thermogenic natural gas emissions can be the major source of excess CH_4 in these urban areas (Brant et al., 2014; McKain et al., 2015; Peischl et al., 2013; Phillips et al., 2013; Townsend-Small et al., 2012; Wennberg et al., 2012). More broadly, CH_4 emissions in cities can also include combinations of multiple fossil fuel sources, as well as biological sources such as waste (landfills, sewers etc.), as seen in studies from Denver, Colorado and Indianapolis, Indiana (Chamberlain et al., 2016; Lamb et al., 2016; Townsend-Small et al., 2016).

Various city studies have focused on detecting and quantifying emission rates from local natural gas distribution systems (Ars et al., 2020; Maazallahi et al., 2020; Von Fischer et al., 2017; Weller et al., 2018). Many of these studies have indicated city emission rates correlate with the state of infrastructure of the local natural gas distribution systems, for example depending on pipeline age and material (Von Fischer et al., 2017; Hendrick et al., 2016; Gallagher et al., 2015). Such studies are useful in targeting infrastructure repairs and replacement plans of the local natural gas distribution systems. Though there are many studies on CH_4 emissions in urban areas, this field of research is still greatly dominated by investigations in U.S. cities. In Europe, studies have focused on only a few cities like London, U.K. (Helfter et al., 2016; Lowry et al., 2001; O'Shea et al., 2014; Zazzeri et al., 2015, 2017), Paris, France (Defratyka et al., 2021; Xueref-Remy et al., 2020), Hamburg, Germany, Utrecht, Netherlands (Maazallahi et al., 2020), and Florence, Italy (Gioli et al., 2012). Less attention has been paid to emissions in eastern European cities (Kuc et al., 2003; Zimnoch et al., 2010, 2018).

Urban CH_4 studies have indicated inconsistencies between measurements and regional inventory budgets. For example, in Boston, natural gas CH_4 emissions inferred from measurements were 2–3 times greater than the current inventory and industrial reports (McKain et al., 2015). Importantly, most local and regional CH_4 inventories do not include top-down (TD) assessments, but instead rely on bottom up (BU) statistical emission estimates. TD methods use measurements of atmospheric CH_4, such as made by aircrafts, vehicles, walkers and tall fixed towers or monitoring stations. TD methods assess emissions integrated over large areas by a variety of techniques such as mass balance methods

(Cambaliza et al., 2014; Mays et al., 2009) and inverse modeling. Continuous mobile measurement techniques and source tracers have been commonly used to investigate CH_4 emissions and identify the sources of these emissions (Defratyka et al., 2021; Lamb et al., 2016; Lowry et al., 2020; Maazallahi et al., 2020; Phillips et al., 2013).

Although, there are often disagreements between TD and BU observations (Saunois et al., 2020), detailed BU measurements can help reconciliate both approaches by detecting street-level emissions and appropriately allocating and quantifying them. This not only helps to reconcile TD and BU budgets, but improved inventories calculations also benefit local municipalities, gas consumers, local distribution companies, and supports resident safety (Han and Weng, 2010; Jackson et al., 2014; Ma et al., 2013). Recently, and currently still ongoing, significant mobile surveying efforts have been made to understand CH_4 sources in European cities. For example, there has been recent European Union and UN supported research in other cities including Paris (Defratyka et al., 2021), Hamburg, Germany & Utrecht, Netherlands (Maazallahi et al., 2020).

Isotope measurements offer potent tools in discriminating between sources. In particular, mobile measurement techniques, in combination with various source tracers, have been efficient at separating emissions between waste sources and fossil fuel sources. Isotopic source signatures depend on the maturity/formation pathway of CH_4 (Schoell, 1984; Whiticar, 1990) (as seen in results section 4.3). Biogenic CH_4 is relatively depleted in ^{13}C and ^2H, whereas thermogenic CH_4, which is produced by the decomposition of ancient organic matter under elevated pressures and temperatures on a geological time scale (Coleman et al., 1981; Schoell, 1988), is often more enriched in ^{13}C and ^2H. CH_4 in air has commonly been analyzed for carbon 13 ($\delta^{13}C_{CH4}$), as a tool in source apportionment. The analysis of δ^2H_{CH4} is becoming more available as technology of analytical sample preparation systems advance, decreasing the need of large sample volumes and analysis time (Fisher et al., 2006; Jackson et al., 1999; Menoud et al., 2020; Röckmann et al., 2016; Yarnes, 2013). Research conducted on the Colorado Front Range in the U.S. has shown that δ^2H_{CH4} was more powerful than $\delta^{13}C_{CH4}$ at distinguishing waste, cattle husbandry, and fossil fuel sources (Townsend-Small et al., 2016). Past studies that have utilized both carbon and hydrogen stable isotopes of CH_4 as source tracers have shown that δ^2H-CH_4 is a more consistent tracer for characterizing natural gas sources (Townsend-Small et al., 2012; 2015; 2016; Maazallahi et al., 2020; Menoud et al., 2021).

The development of cavity ring-down spectroscopy (CRDS) and the capability of faster analysis (compared to isotopic analysis) has led to the utilization of ethane (C_2H_6):CH_4 ratios (C_2:C_1) (Lowry et al., 2020; Maazallahi et al., 2020; Yacovitch et al., 2014), which allows for real-time determination of emission sources. C_2:C_1 ratios have been measured to identify gas leaks from natural gas distribution systems in cities (Lamb et al., 2016; Maazallahi et al., 2020; Wunch et al., 2016), since biogenic sources do not contain C_2 higher alkanes, like C_2H_6, which are found only in thermogenic or combustion sources (Clayton 1991; James 1983). Past studies of pipeline material and age of a natural gas distribution network have shown that it is possible to model a network's "leak potential", with old cast iron and unprotected steel pipelines being most susceptible to corrosion, and thus with a greater frequency of leaks per unit of pipeline length (Harrison et al., 1996 Jackson et al., 2014; Lamb et al., 2015; Phillips et al., 2013; Von Fischer et al., 2017). These findings have also indicated that cities with aggressive pipeline repairs and replacement programs have fewer leaks per mile (90% less) when compared to cities without such maintenance programs (Gallagher et al., 2015).

Romania's long-standing oil and gas industry, the emergence of Bucharest as a major metropolis, and the lack of street-level measurements from Eastern European cities all make this region an interesting study site. Romania has a complex geological history resulting in an abundance of hydrocarbon-rich reservoirs within the Pannonian-Transylvanian Basin (Cranganu and Deming, 1996) and the

Carpathian-Balkanian Basins (Amadori et al., 2012; Sclater et al., 1980). In 2019, Romania's natural gas production was 9.7 billion cubic meters, making Romania the 4th largest natural gas producer in Europe (BP, 2020). Romania's economy has long thrived from the petroleum industry due to the country's high producing reservoirs and was the first country to export gas in the 1900's (Nita, 2018). In 2016, Romania ranked within the top 20 countries globally for the reported highest gas-related CH_4 emissions globally (0.21 Tg a^{-1}) (Scarpelli et al., 2020).

This study aims to gain an understanding of urban street-level CH_4 emissions in Bucharest, Romania by answering the following questions:

1) What is the total annual CH_4 city-wide emission rate?
2) What are the dominant sources contributing to these emissions? and
3) How does the distribution of CH_4 sources in Bucharest compare with other measured cities?

To answer these questions, mobile surveys were conducted in the urban areas of Bucharest while continuously measuring CH_4 and C_2H_6 for locating enhanced CH_4 mole fractions above local atmospheric background, which are referred to as a leak indication (LI). The flux rates were determined for identified clusters of LIs. An annual city wide total emission estimate was calculated by scaling up the flux rates. Multiple locations, where CH_4 exceeded the daily atmospheric background mole fractions, were measured for $\delta^{13}C_{CH4}$, δ^2H_{CH4}, and C_2:C_1 ratios for tracing contributing CH_4 sources. As Europe seeks to cut urban emissions, studies like this will be useful for identifying targets for mitigating emissions and for assessing future governmental regulation of greenhouse gas (GHG) emissions.

2. Study location

The focus location of this research is Romania's capital city, Bucharest. Romania has an area of 238,397 km^2 and a population of 19.4 million people in 2019 (National Institute for Statistics, 2020). Bucharest is in the southeast of the country (44.4325° N, 26.1039° E). The metropolitan area covers 1811 km^2, with a population of 2.2 million people in 2019 (National Institute for Statistics, 2020). In addition to Bucharest, we also surveyed the nearby urban city of Ploiești, the historic center of Romania's oil industry, which is located in the county of Prahova, ~60 km north of Bucharest (44.9333°N, 26.0333°E). Ploiești is much smaller by comparison, covering about 58 km^2 with a population of 225,000 (National Institute for Statistics, 2020).

The total reported GHG emissions of Romania in 2018 were equivalent to 116,115 kt CO_2, which is made up of 66% CO_2, 24% CH_4 (28,184 kt CO_2 eq), 7% N_2O, and less than 2% fluorinated gases (Deaconu, 2020). The energy sector accounts for 66% (77,006 kt CO_2 eq) of the annual emissions, agriculture is 17%, industrial processes are 12%, and 5% is from the waste sector. These total relative GHG proportions are broadly similar to those from 1989, although the declared total fugitive CH_4 emissions from fossil fuels/distribution and livestock have decreased by 62% (UNFCCC, 2019). CH_4 emissions reported to the UNFCCC showed a 61.22% decrease between 1989 and 2017 (UNFCCC, 2019). From 1989 to 1992, decreased coal mining and lower energy consumption significantly reduced GHG emissions. The commissioning of Romania's Cernavodă Nuclear Power Plant 1996 has influenced a decrease in emission estimates from the energy sector.

Bucharest's industry, society, and landscape has been changing rapidly since the early 1990's and the city's economy has been growing since joining the EU framework (Nae and Turnock, 2011; Zolin, M.B., 2007). The 1989 Romanian Revolution and the resulting change of territorial governance practices had significant impacts on the management of Romania's urban GHG emissions (Kilkiş, Ş., 2016), including the development of Bucharest's urban landscape and municipal planning (Ianoş et al., 2016, 2017; Nae and Turnock, 2011). During early 2004, Romania published its first National Waste Management Strategy (Orlescu and Costescu, 2013). Up until 2009, when the European model

of integrated waste management was adopted, villages were storing waste in unofficial storage locations (Orlescu and Costescu, 2013). After the EU accession, Bucharest has closed 29 landfills (non-complying) and now has 3 major landfills (Chiajna-Rudeni, Glina and Vidra) located on the outskirts of the urbanized area (Orlescu and Costescu, 2013; Ianoş et al., 2012). Before the Glina Wastewater Treatment Plant was implemented in 2011, Bucharest did not have a designated wastewater treatment facility (Peptenatu et al., 2012; Veolia, 2013; Bojor, 2010), and raw wastewater was directly discharged into the local rivers (Arges, Dambovita and Colentia) (Peptenatu et al., 2012). The total simple length of sewage pipeline within Bucharest Municipality was 3657 km in 2019 (National Institute for Statistics, 2020), which collects both wastewater and storm water that discharges into a main conduit under the Dambovita River (Gogu et al., 2017). Both landfills and the sewage network are large potential contributors to the waste sector CH_4 emissions. Within the Bucharest municipality boundary, there was ~2124 km of gas pipeline contributing to the natural gas distribution network in 2019 (National Institute for Statistics, 2020), which may be a large source of fossil fuel CH_4 emissions.

Although Romania does have a framework law on waste, Ianos et al. (2016; 2017) suggest that Bucharest has lacked urban planning policies due to the passive urban management by local and central authorities. Measuring and monitoring GHG emissions in Bucharest may aid the local city governance to prioritize and enforce policies for the maintenance of municipality infrastructure such as natural gas distribution pipelines, residential and industrial sewage systems, and larger waste facilities like landfills (Iacoboaea and Petrescu 2013; Alamsi, 2013; Ianoş et al., 2012; Sandulescu, 2004).

3. Methods & materials

3.1. Mobile set-up

3.1.1. Continuous instruments

Street-level emissions were measured using three vehicles and four different continuously measuring CRDS instruments. This included a Picarro G2301 (CH_4, CO_2, and H_2O) and a Picarro G2401 (CH_4, CO, CO_2, and H_2O) instrument. Both the G2301 and G2401 analyzers measure at a frequency of 0.33 Hz, and have a flow rate between 260 and 400 mL min^{-1} (Picarro, 2017a, 2019). Since C_2H_6 is a major component present in natural gas sources, two CRDS instruments were used to aid in source identification and attribution, measuring mole fractions of CH_4, C_2H_6, and H_2O; a Picarro Gas Scouter TM G4302 (Picarro, 2017b) and a Los Gatos Research Ultraportable CH_4/C_2H_6 Analyzer (LGRUMEA). The G4302 analyzer was measuring both CH_4 and C_2H_6 at 1 Hz at a flow rate of ~2 L min^{-1}. The LGRUMEA has a standard flow rate of 1.7 L min^{-1} and was set to measure at 0.5 Hz. To ensure accuracy and comparability of the different continuous measurements, instruments measured gas standards, from MPI Jena, which were calibrated to the NOAA WMO X2004A CH_4 scale before and after the campaign. A cylinder tank containing 1 ppm C_2H_6 was also used for reliable C_2:C_1 measurements on the LGRMEA. The Picarro G4302 was cross calibrated using a 6.5 and 80 ppm CH_4 dilutions from a cylinder containing a 3.9% C_2:C_1 ratio, which was verified by the local gas company in Utrecht (STEDIN). A linear regression was produced from each of the instrument's calibration measurements vs. assigned mole fractions, and was applied to correct the raw data.

3.1.2. Sampling details

Non-electric vehicles were equipped as a mobile sampling kit. Supplied to each vehicle was an additional battery that was connected to the engine to power the instruments, an external sampling inlet, and equipment for recording location and wind parameters. The sampling inlet tube led from the vehicle's front bumper to the interior of the rear trunk, where it was connected to the intake valve of an instrument. If there were 2 instruments or a sampling pump in the car, a splitter was

added for the instruments and the sampler pump to pull air from the same inlet. The sampling inlet was secured 60 cm from the ground level of each car. The average inlet delay for each instrument was as follows: G2301 at 17 s, G2401 at 5 s, G4302 at 5 s, and the LGRUMEA at 10 s. All vehicles had a GPS unit and an anemometer that recorded coordinates and wind speed and direction every second. Live data recordings were displayed either with a netbook, tablet, or monitor via internal Wi-Fi with ethernet or virtual network computing (VNC) connection.

Air samples were collected for analysis of stable carbon and hydrogen isotopic compositions of CH_4. A 12 V battery powered micro-diaphragm gas pump was attached to the sampling inlet via a splitter, or attached to an additional inlet that was in line with the instrument sampling inlet. A half-inch stainless steel dryer tube (magnesium perchlorate) was attached after the gas pump to limit the amount of moisture in the air sample. During the surveys, Flexfoil SKC and Supelco bags (3 L) were manually filled by a passenger within the vehicle. Each air sample took about 30 s to fill.

3.1.3. Survey strategies and sampling procedures

The main city campaigns for Bucharest and Ploiești were conducted in the late summer of 2019. A total of 27 surveys split between three vehicles were carried out in Bucharest between the 20th and 29th of August. The additional surveys of Ploiești were conducted (September 2-5, 2019), and utilized one car and only the G2401 analyzer. The equipment time clocks were synchronized to local time at the start of the day to facilitate matching of parameters between instruments. All surveys were about 6–8 h in duration and were carried out during daylight hours.

Air samples for isotopic analysis were collected both downwind and upwind of plumes. Generally, spot sampling took place during the last 2 days of the main Bucharest campaign (28th – 29th Aug) and the last day of the Ploiești campaign (Sep 5th). During October of the same year, there were two additional days (16th and 18th) of sample collection from Bucharest and one day (15th) from Ploiești. Locations were targeted based on the August surveys and the presence of LIs, and by known local waste sources (landfills and sewage treatment plants). This was to collect samples for additional isotopic analysis. If time and locality allowed, the vehicle was parked to trace the exact locality of the source of a LI. This was done by attaching an extension tube (5–8 m) to the instrument intake inlet on the bumper, then walking around with a mobile device to read the measurements from the surrounding infrastructure (e.g. manholes, storm drains, residential gas meters, and above ground pipelines).

3.2. Data and sample processing

3.2.1. CH_4 leak indication quantification & emission calculations

CH_4 leak indication quantifications and flux rates were determined from the continuous CRDS measurements and data recorded within the city boundary. Here we utilized an algorithm that was initially developed by Von Fischer et al. (2017), later improved by Weller et al. (2019) and modified by Maazallahi et al. (2020). Von Fischer and Weller utilized this methodology to detect and quantify street level leaks from natural gas distribution networks from continuous mobile measurements. Maazallahi et al. (2020) broadened this methodology to include additional street-level emissions from other non-fossil fuel sources, which was applied to two European cities studies (Hamburg, Germany, and Utrecht, Netherlands). Similarly, Defratyka et al., 2021 applied this methodology to 2018 and 2019 measurements of Paris, France.

For this study, the local atmospheric background CH_4 mole fraction is defined as the CH_4 mole fraction baseline. Specifically, we used a mean time frame of ± 2.5 min as an averaging moving window applied before and after each individual measurement. Subtracting the baseline mole fraction from the measurements allows us to determine where the CH_4 mole fraction exceeds the baseline (CH_4 excess). Here, we define any CH_4 excess ≥ 0.2 ppm above the CH_4 mole fraction baseline as a CH_4

leak indicator (LI).

Two speed limits were applied to exclude either unintended or unreliable measurements. All CH_4 LIs recorded at a speed of zero (mostly while stopped in traffic) were excluded to avoid any unintended signals from natural gas fueled vehicles and interference from general vehicle exhausts (Maazallahi et al., 2020). A past controlled release test verified that instrument performance at high speeds deviate outside of the recommended operation ranges, resulting in unreliable CH_4 measurements (Von Fischer et al., 2017; Weller et al., 2019). Therefore, CH_4 LIs recorded at speeds >70 km h^{-1} were excluded from leak quantification. All CH_4 LIs were time aggregated (5 s) and spatially clustered based on the algorithm constraints. Within this time window, the LIs are added and are treated as a single source leak. This defines the final CH_4 LI location of the cluster. CH_4 emission rates are quantified for each cluster using an empirical equation defined in Weller et al. (2019).

$$\overline{\ln(C)} = -0.988 + 0.817 * \ln(Q) \qquad (1)$$

where C represents the maximum CH_4 LI (ppm) above the CH_4 mole fraction baseline, and Q is the estimated CH_4 emission rate in L min^{-1}. Where there were multiple passes for one location, the average $ln(C)$, based on the respective maximum CH_4 values of each pass, was used in the left side of equation (1) to calculate the emission rate (as in Weller et al., 2019).

To calculate a citywide CH_4 emission rate, the sum of the flux rates was converted from L min^{-1} to units of mass time[-1] using the relative density of CH_4 gas at 25 °C, 1 atm. The emission factor (EF) for scaling up is the sum of all measured city emissions divided by the distance covered. This was then multiplied by the total length of streets within the metropolitan boundary of the study location, and then converted to metric tons of CH_4 per year for an annual city estimate. The uncertainty is calculated from a non-parametric bootstrap emission estimate that scales up the total number of LIs (after clustering) to account for the whole city. This process resamples the LIs 30,000 times. The mean of the iterated estimates is similar to the calculated annual city-wide emission rate, and the uncertainty is the range (min and max). Further details are described in Maazallahi et al. (2020).

3.2.2. Isotopic measurements

Air samples were distributed either to Royal Holloway University of London (RHUL) or Utrecht University (UU) for CH_4 mole fraction and isotopic analyses. If enough sample air remained in a bag after analysis, then the sample was exchanged between the UU and RHUL for duplicate $\delta^{13}C_{CH4}$ measurements. Samples measured at the RHUL department of Earth Sciences Greenhouse Gas Laboratory were first analyzed for CH_4 mole fractions using a Picarro G1301 CRDS analyzer, which logged data every 5 s for 2 min resulting in a precision ± 0.3 ppb (Lowry et al., 2020; France et al., 2016; Zazzeri et al., 2015). RHUL samples were then measured for stable isotopes ($\delta^{13}C_{CH4}$) using a high precision (± 0.05‰) Elementar Trace Gas continuous-flow gas chromatograph isotope ratio mass spectrometer (CF GC-IRMS) system (Fisher et al., 2006). Each sample was measured 3 or 4 times for $\delta^{13}C_{CH4}$ to achieve the desired precision. Both RHUL instruments are calibrated weekly to the WMO X2004A CH_4 scale using air-filled cylinders that were measured by the National Oceanic and Atmospheric Administration (NOAA), and cylinders that were calibrated against the NOAA scale by the Max-Planck Institute for Biogeochemistry (MPI-BGC) Jena (Lowry et al., 2020; France et al., 2016; Zazzeri et al., 2015; Fisher et al., 2006).

Air samples measured at the Institute for Marine and Atmospheric Research Utrecht (IMAU) at UU were analyzed for both $\delta^{13}C_{CH4}$ and $\delta^{2}H_{CH4}$ using a ThermoFinnigan MAT DeltaPlus XL, Thermo Scientific, coupled to a sample preparation system described previously (Brass and Röckmann, 2010). This IRMS system has a precision of 0.1‰ for $\delta^{13}C_{CH4}$ and 2.0‰ for $\delta^{2}H_{CH4}$ (Menoud et al., 2020; Röckmann et al., 2016). Each final isotopic value is an average of 2–4 measurements. The IMAU measurements are converted to international isotope scales using known

reference air cylinders that were calibrated against standards from MPI-BGC, Jena, Germany (Sperlich et al., 2016).

3.2.3. $\delta^{13}C_{CH4}$ and δ^2H_{CH4} source signature calculations

$\delta^{13}C_{CH4}$ and δ^2H_{CH4} source signatures were calculated using the Keeling plot technique (Keeling, 1958, 1961). This calculates the linear regression between the measured delta value ($\delta^{13}C_{CH4}$ or δ^2H_{CH4}) and the inverse mole fraction ($[CH_4]^{-1}$) of the air samples, where the y-intercept represents the estimated source signature (Keeling, 1958, 1961; Pataki et al., 2003). This signature indicates the dominant CH_4 source that has increased the background CH_4 mole fraction. To calculate the y-intercept, we use the Bivariate Correlated Errors and intrinsic Scatter (BCES) regression to account for both the differences in the x and y axes, as well as accounting for the measurement errors (Akritas and Bershady, 1996). This technique has been utilized by many recent studies (Lowry et al., 2020; Xueref-Remy et al., 2020; Zazzeri et al., 2016, 2017) and further details are described in Zazzeri et al. (2015) and France et al. (2016).

3.2.4. Ethane-methane ratio (C_2:C_1) source determination

The C_2:C_1 ratio is a useful diagnostic for gas leak attribution because C_2H_6 is present in measurable quantities in thermogenic gas, but not in biogenic gas (e.g. Plant et al., 2019). Knowledge of the C_2:C_1 ratio for the local gas supply allows emissions captured during the surveys to be compared to the expected signature for a local gas leak. For the two instruments with C_2H_6 measurements, the data were first smoothed using a 5 s moving average window for both C_2H_6 and CH_4 to reduce baseline noise. Data points with a CH_4 LI ≥ 0.5 ppm and ≥ 3 ppm (for the Picarro and LGR analyzers, respectively) were then selected, and the C_2:C_1 ratio calculated using a linear regression over a 10 s window centered around each CH_4 LI point. For these LIs, the corresponding C_2H_6 measurement would be above the baseline noise of the respective instrument at a C_2:C_1 ratio of 0.01, ensuring that thermogenic signals are not misclassified as biogenic. This is further discussed in section 4.4.

4. Results

4.1. CH_4 mole fractions and leak indications

SI Fig. 1 displays the total roads driven and spatial coverage of CH_4 excess, indicating localities where CH_4 is greater than the atmospheric baseline. SI Fig. 1 shows that CH_4 LIs detected within the city area are mostly narrow plumes, but there were wide plumes identified just northwest of the Bucharest boundary, located close to Chiajna-Rudeni landfill site. Northeast of the city boundary, the largest CH_4 LIs were found on a residential road, Drumul Potcoavei (Horseshoe Road) (44.505°N, 26.133°E), 410 m outside the Bucharest city border. The highest LGRUMEA reading at this location was around 650 ppm CH_4 and 30 ppm C_2H_6. Upon returning the next day with the local gas company, the G4203 recorded the highest mole fraction above background (around 2070 ppm CH_4 and 49 ppm C_2H_6). These extremely high values are above the instrument saturation point, therefore these are not necessarily accurate. The maximum was measured while trying to find the exact leak location on foot, therefore these data were at zero speed and not used for emission evaluations. This specific CH_4 leak indication was confirmed as a natural gas pipeline leak by the local utility company, which allowed for the characterization of the representative isotopic source signatures and C_2:C_1 ratio of the natural gas distribution network.

4.2. CH_4 leak indications and emission rates

Emission quantification and analysis is summarized in Table 1. The spatial distribution of the accepted CH_4 LI clusters can be seen in Fig. 1. It should be reminded that these locations represent CH_4 emissions from any source, not just gas pipelines. From the distance covered in Bucharest, 2482 CH_4 LIs were identified which were clustered into 969 LI locations, where the maximum CH_4 excess was 38 ppm (mean = 1 ppm $\pm$ 0.1 s.e.) (Table 1). Of these locations, the maximum inferred
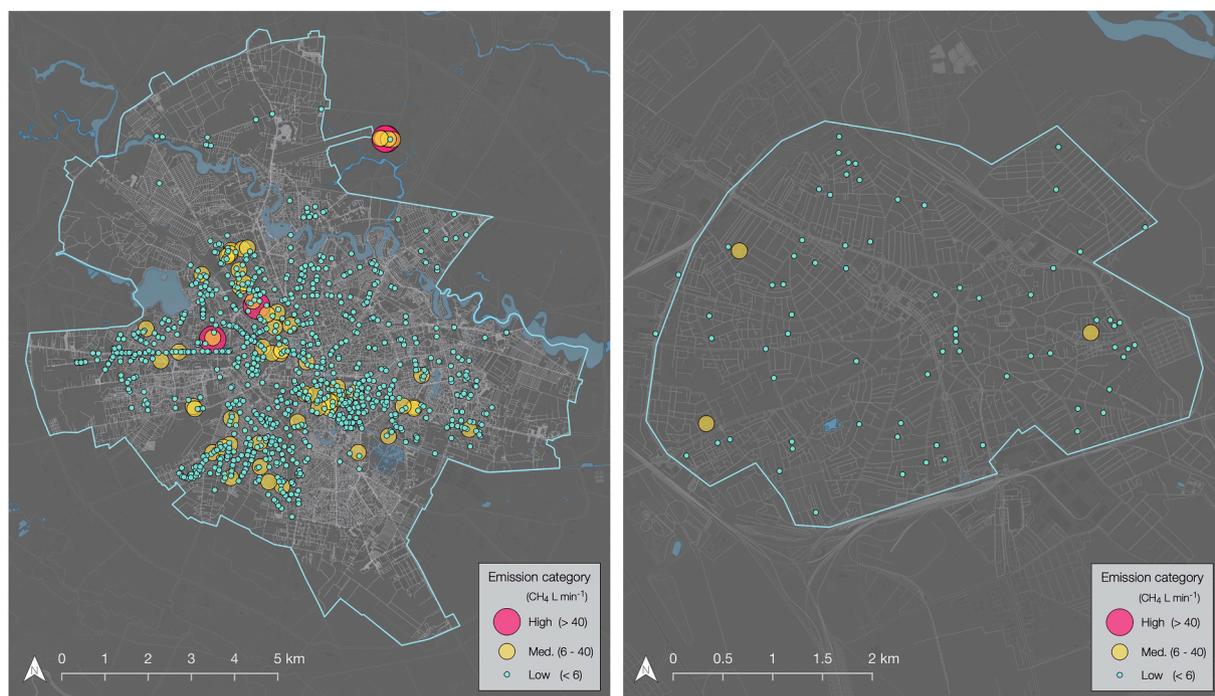

Fig. 1. Methane emission rate categories of Bucharest and Ploieşti. Bucharest (left) has 969 CH_4 LI localities that were identified through clustering a total of 2482 CH_4 LIs. The major Drumul Potcoavei leaks (northeast of the Bucharest boundary) include 7 LI locations which were clustered from 89 CH_4 indicators. Ploieşti (right) includes CH_4 76 LI locations, clustered from 87 CH_4 LIs. Within the city borders (solid blue line), the maximum averaged emission rate was 45 L min^{-1} for Bucharest and 15 L min^{-1} for Ploieşti. Magnitude categories defined as in von Fisher et al., 2017. The corresponding data are summarized in Table 1. (For interpretation of the references to color in this figure legend, the reader is referred to the Web version of this article.)

Table 1
Summary of emission quantifications and analysis. Survey distances (excludes multiple passes), CH$_4$ leak indications and clustered locations, CH$_4$ emission rates of measured leaks, standard errors (s.e.) for uncertainties, and emission categories.

		Statistic	Bucharest	Ploieşti	Drumul Potcoavei
Distances	driven (km)	N	1845	240	–
	covered (km)	N	1359	233	–
CH$_4$ leak indications (LIs)	LIs	N	2482	87	89
	LI cluster locations	N	969	76	7
	density (locations km^{-1})	P	0.71	0.33	–
	CH$_4$ excess (ppm)	Max	38.3	38.2	397.1
		Mean	0.9	1.1	69.0
		Median	0.4	0.4	15.9
		s.e.	0.1	0.5	54.8
CH$_4$ emissions	rates (L min^{-1})	Sum	2124.0	138.8	532.6
		Max	44.5	14.7	365.7
		Mean	2.2	1.8	76.1
		Median	1.1	1.0	17.4
		s.e.	0.1	0.3	50.1
	factor (L km^{-1} min^{-1})	EF	1.6	0.6	–
Emission category	LI locations small <6 (L min^{-1})	(n) emission sum	913 1322	73 106	1 5
	LI locations medium 6–40 (L min^{-1})	(n) emission sum	54 713	3 33	2 56
	LI locations high >40 (L min^{-1})	(n) emission sum	2 89	– –	5 5880

Note: reported max and min leak indications are for single passes, but the emission rates are estimated based on averaging the (LIs of multiple passes) as in equation (1). Driven distance is the total driven throughout the entire campaign, where the covered distance is only the distance driven within the Bucharest city boundary.

emission rate was 45 L min^{-1} (mean = of 2 L min^{-1} ± 0.1 s.e.; n = 969). Dividing the number of clustered LI locations in Bucharest by the road coverage determines a CH$_4$ LI density of 0.7 (LIs per km covered). Using the same distance, the final emission factor calculated was 1.6 L km^{-1} min^{-1} (Table 1).

In Ploieşti, 87 CH$_4$ LIs were detected within the 233 km of road covered, which account for 76 CH$_4$ LI cluster locations (Table 1). Similar to Bucharest, maximum excess of measured leaks in Ploieşti was also 38 ppm CH$_4$ (1 ppm ± 1 s.e; n = 76). Ploieşti's maximum averaged emission rate found was 15 L min^{-1} (mean = 2 L min^{-1} ± 0.3 s.e.). Taking the total number of clustered CH$_4$ LIs to the total road distance covered, calculates a CH$_4$ LI density of 0.3 (LIs km^{-1}) and an emission factor of 0.6 L km^{-1} min^{-1}.

On Drumul Potcoavei (the road mentioned above, outside Bucharest city limits, with a large gas pipeline leak), CH$_4$ LIs were observed near continuously over a distance of 0.7 km. A total of 89 CH$_4$ LIs were detected and contribute to the 7 LI cluster locations. The maximum CH$_4$ excess was 397 ppm (mean = 69 ppm ± 55 s.e.; n = 7). Along this transect, the largest averaged emission rate found on this single road was 366 L min^{-1} (mean = 76 L min^{-1} ± 50 s.e.; n = 7), and the total sum of all the averaged emissions was 533 ± 50 L min^{-1}.

To categorize the CH$_4$ LI emission rates, we utilize the emission magnitude categories defined in von Fisher et al., 2017, which defines a "small" leak rate as < 6 L min^{-1}, a "medium" leak is between 6 and 40 L min^{-1}, and any leak ≥40 L min^{-1} is considered "high" (Fig. 1, Table 1). The total emissions from Bucharest are defined as 62% small, 34%

medium, and 4% large, and Ploiesti's total emissions were 76% small and 24% medium (SI Fig. 2). For Drumul Potcoavei, 1% of the emissions were small, 11% were medium and 89% were large (SI Fig. 2).

4.3. Isotopic source signatures

Isotopic measurements between the RHUL and UU laboratories are in good agreement, indicated by an average difference of duplicate $\delta^{13}C_{CH4}$ source signature calculations of ±0.32‰ (n = 11) (SI Fig. 5). For Bucharest, a total of 45 locations were sampled for the stable isotopic composition of CH$_4$ (δ^2H_{CH4} and $\delta^{13}C_{CH4}$), and 8 locations were sampled in Ploieşti. For both cities, two of the locations were sampled more than once. The results summaries of isotopic source signatures are shown in SI Tables 1 and 2 Since our sample set of Ploieşti is 20% smaller than the sample size of Bucharest, we combine the city data for a general isotopic urban analysis. To minimize potential skewing of analysis from the offset of the number of $\delta^{13}C_{CH4}$ (n = 58) and δ^2H_{CH4} (n = 56) source signatures, only one $\delta^{13}C_{CH4}$ source signature was used for each sampled location.

$\delta^{13}C_{CH4}$ source signatures ranged from -61‰ to -36‰ (mean = -49 ± 6‰ s.d.; n = 55), and δ^2H_{CH4} ranged from -388‰ to -157‰ (mean = 274 ± 69‰ s.d.; n = 55). The known source type signatures are indicated by an asterisk in SI Tables 2 and 3 and displayed in Fig. 2. Sources falling under an 'unknown' type have either ambiguous signatures where $\delta^{13}C_{CH4}$ and δ^2H_{CH4} are not in agreement of source type or the signature falls in the overlapping range between thermogenic and biogenic, and the exact location of the source could not be found.

For known thermogenic natural gas signatures, our end member sample was confirmed by the local natural gas company. This was the leak found on Drumul Potcoavei which was sampled with the assistance of the natural gas company by opening up a utility access panel (manhole) (SI Fig. 3). The $\delta^{13}C_{CH4}$ source signatures of this leak ranged from -51‰ to -47‰ (mean = -49‰ ± 2 s.d., n = 4) and δ^2H_{CH4} signatures ranged from -175‰ to -132‰ (mean = -154‰ ± 31 s.d.; n = 2). All known fossil fuel source signatures have a $\delta^{13}C_{CH4}$ mean of -50‰ ± 5 s.d. (n = 8) and a δ^2H_{CH4} mean of -188‰ ± 40 s.d. (n = 8). The most depleted $\delta^{13}C_{CH4}$ fossil fuel signature was -60‰, which was directly sampled from a domestic gas supply box (SI Fig. 4) in Ploieşti and had a δ^2H_{CH4} signature of -198.4‰ (Table 3, source P-9c). The $\delta^{13}C_{CH4}$ values are much more depleted compared to other natural gas leaks we found in Bucharest.

For biogenic waste signatures, Vidra-Sinteşti landfill and Glina-Popeşti-Leordeni landfill in southern and eastern Bucharest were sampled downwind. These measurements resulted in a known landfill signature of $\delta^{13}C_{CH4}$ = -58‰ ± 1 s.d. (n = 2) and δ^2H_{CH4} = -280‰ ± 6 s.d. (n = 2). For a known wastewater signature, Glina water treatment plant was targeted and sampled downwind which resulted in a $\delta^{13}C_{CH4}$ of -50‰ and a δ^2H_{CH4} of -335‰ (SI Table 1).

The spatial distribution of the city samples, analyzed for both $\delta^{13}C_{CH4}$ and δ^2H_{CH4}, are shown in Fig. 3. There is an overlap in $\delta^{13}C_{CH4}$ isotopic signatures for the known gas and wastewater samples, but better separation of the δ^2H_{CH4} signatures, indicated by more color variability (Fig. 3). This is further supported by the bi-modal δ^2H_{CH4} distribution vs the normal distribution of the carbon signatures (Fig. 4). There is a large cluster of biogenic δ^2H_{CH4} signatures, implying that local wastewater emissions may be responsible for many of the CH$_4$ LIs identified.

4.4. Ethane:methane (C$_2$H$_6$:CH$_4$) ratios

Ethane:methane (C$_2$:C$_1$) ratios were calculated as an additional source tracer. Ratios were calculated where CH$_4$ leak indications were >0.5 ppm (for the Picarro G4302 analyzer) and >3 ppm (for the LGR UMEA analyzer) above the local CH$_4$ baseline. In total 11% of the LIs could be attributed to sources using this technique and may not be representative of the smaller LIs which fall below the detection limits.
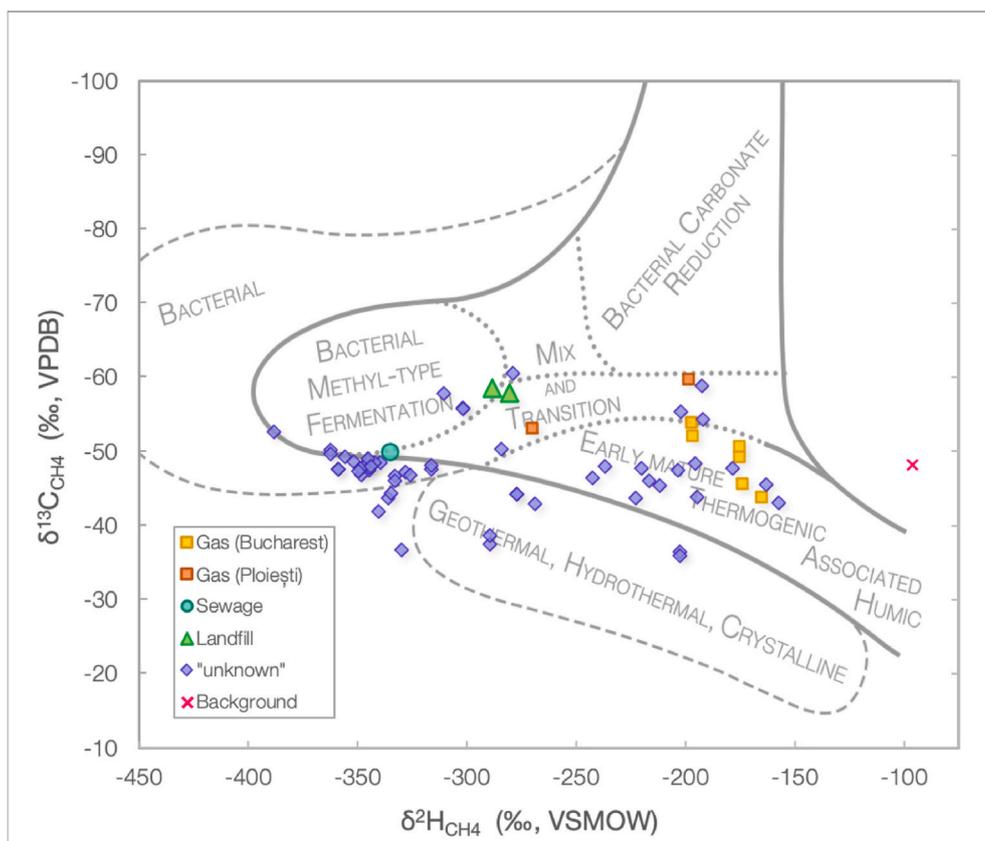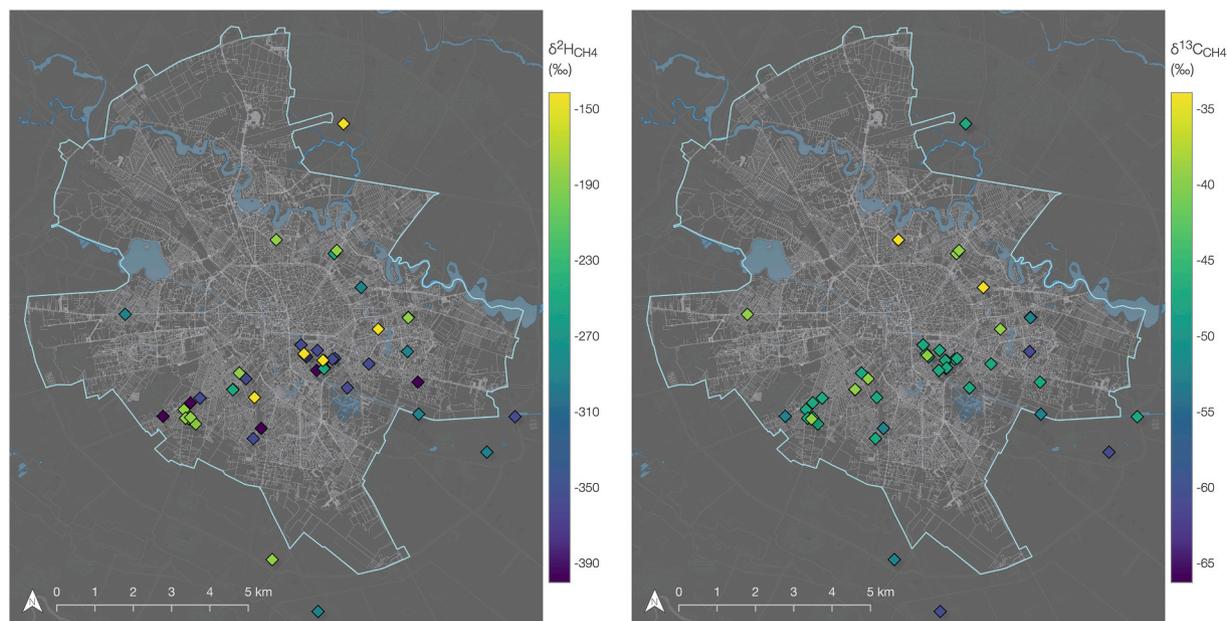
Fig. 2. Isotopic source signatures of enhanced CH₄ where bag samples were collected. Comparison between 11 identified and 55 unknown (purple diamond) source signatures. Known $\delta^{13}C_{CH4}$ source signature ranges: gas -60 to -44‰ (yellow & orange, n = 5), landfill -59 to 58‰ (green triangle, n = 2), and wastewater is -50‰ (circle). Known $\delta^{2}H_{CH4}$ source signature ranges: natural gas -270 to -166‰, landfill -288 to -280‰, and wastewater is -335‰. Points overlay bacterial and thermogenic classifications from Whiticar, 1990). (For interpretation of the references to color in this figure legend, the reader is referred to the Web version of this article.)

Fig. 3. Spatial distribution of $\delta^{13}C_{CH4}$ and $\delta^{2}H_{CH4}$ source signatures. Combined RHUL and UU $\delta^{13}C_{CH4}$ signatures (left), yellow colors indicate sources of ^{13}C enrichment and blue colors show ^{13}C depletion. $\delta^{2}H_{CH4}$ signatures (right), yellow colors are more enriched and are indicative of thermogenic sources, and purple darker shades indicate ^{2}H depletion and are more likely to be biogenic sources. Signatures correlate to values and locations listed in SI Table 1. Less source signature overlap for $\delta^{2}H_{CH4}$ is indicated by the greater color variability. (For interpretation of the references to color in this figure legend, the reader is referred to the Web version of this article.)

The spatial distribution and locations of Bucharest C_2:C_1 ratios is shown in Fig. 5, where the maximum C_2:C_1 ratio was 0.300 (mean = 0.02 ± 0.004 s.e.; n = 111). This shows a larger dataset and more uniform spread of measurements than the isotopic data. The light yellow colored points are expected to represent biogenic CH₄ emissions (mainly wastewater) and those with C_2:C_1 ratios above 0.01 are representative of gas pipeline or combustion emissions (orange and darker colors). The leak on Drumul Potcoavei road had measured C_2:C_1 ratios of 0.016,
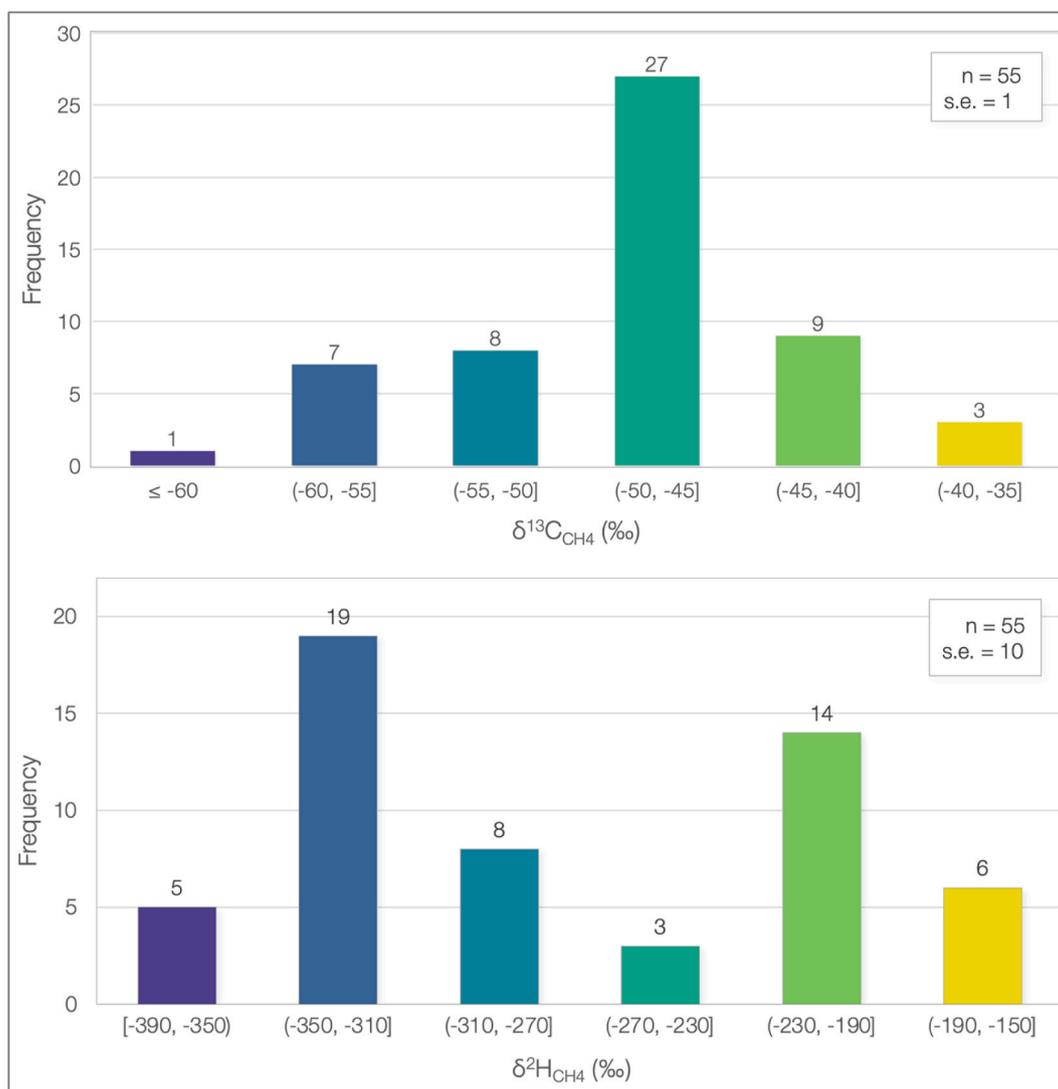
Fig. 4. City source signature population distribution ($\delta^{13}C_{CH4}$ and δ^2H_{CH4}). Combined source signatures of both Bucharest and Ploieşti. Histogram showing a unimodal distribution of $\delta^{13}C_{CH4}$ (top) signatures ranging from -65‰ to -37‰. δ^2H_{CH4} source signatures (bottom) show a bimodal distribution ranging from -388‰ to -157‰. 6% of LIs were attributed to sources using δ^2H_{CH4} source signatures. Colors correspond to the color scale in Fig. 3. (For interpretation of the references to color in this figure legend, the reader is referred to the Web version of this article.)

0.018, and 0.022, which are in agreement with a fossil fuel origin. Within the plume near Chiajna-Rudeni landfill site there was no C_2H_6, as expected from biogenic waste sources.

Fig. 6 is a histogram showing the population distribution of the calculated $C_2:C_1$ ratios. The maximum $C_2:C_1$ ratio was 0.300 (mean = 0.02 ± 0.004 s.e.; n = 111). For this study we define our $C_2:C_1$ source type ratios based on past studies, where biogenic sources ratios range from anything <0.005, thermogenic sources range from >0.005 to <0.09, and a ratios >0.10 are considered pyrogenic or combustion (Defratyka et al., 2021; Kort et al., 2016; Lowry et al., 2020; Yacovitch et al., 2014, 2020; Sherwood et al., 2017). Using these ranges, our $C_2:C_1$ dataset is 63% biogenic (wastewater), 32% identify as thermogenic (fossil fuel), and 5% indicate other/pyrogenic origins (Table 2). From Fig. 6, gives us a visual of the of how the $C_2:C_1$ dataset is dominantly more biogenic, which are most likely from wastewater. Some plumes were traced back to manholes or storm grates that expose the sewage pipelines to the atmosphere. Landfills were outside of the city boundaries and were not included in this apportionment. Due to instrument limitations, Ploieşti surveys were conducted without an C_2H_6 analyzer.

5. Discussion

5.1. City wide methane emissions estimations

We calculated an annual city-wide emission rate for both Bucharest and Ploieşti. To scale-up the city emissions, we used an emission factor of 1.6 L min^{-1} km^{-1} for Bucharest and 0.6 L min^{-1} km^{-1} for Ploieşti, respectively (Table 1). By scaling-up Bucharest's emissions to the entire road network (3399 km) (National Institute for Statistics, 2020) within the Bucharest city boundary, we estimated an annual emission of 1832 tons CH_4 yr^{-1} (min = 1577 t yr^{-1} and max = 2113 t yr^{-1}) (assuming this is representative of emissions throughout the year) or ~45,800 tons CO_2 – equivalent (CO_2-e), using a CH_4 GWP of 25 (U.S. EPA, 2020). Ploieşti's emission rate scaled-up to 324 km of city roads is 67 tons CH_4 yr^{-1} (min = 43 t yr^{-1} and max = 110 t yr^{-1}) or ~1675 tons CO_2-e (U.S. EPA, 2020).

The annual emission rate of Bucharest is much larger than recently surveyed European cities. A study conducted in 2018 by Maazallahi et al. (2020) estimated an annual emission rate (440 ± 70 tons CH_4 yr^{-1}) for Hamburg, Germany (~ 1.45 million people) that is 24% of the estimated emissions of Bucharest. Defratyka et al. (2021) surveyed the city of Paris, France (~ 2 million people) between autumn 2018 –
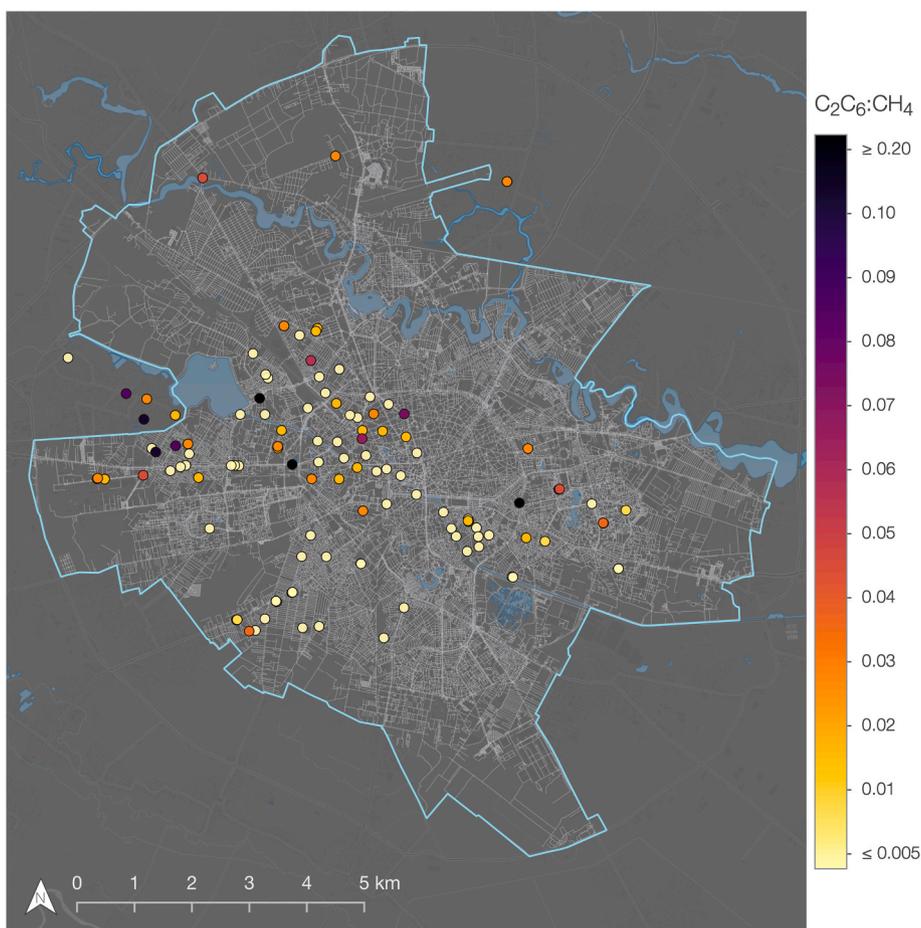
Fig. 5. Bucharest ethane:methane spatial distribution. C_2:C_1 ratios calculated, where peaks of >0.5 ppm and >3 ppm CH_4 excess over background (for the Picarro G4302 and LGR UMEA analyzers, respectively) were recorded. Lighter colors indicate a relatively low abundance of C_2H_6 and darker shades a relatively high abundance. (For interpretation of the references to color in this figure legend, the reader is referred to the Web version of this article.)
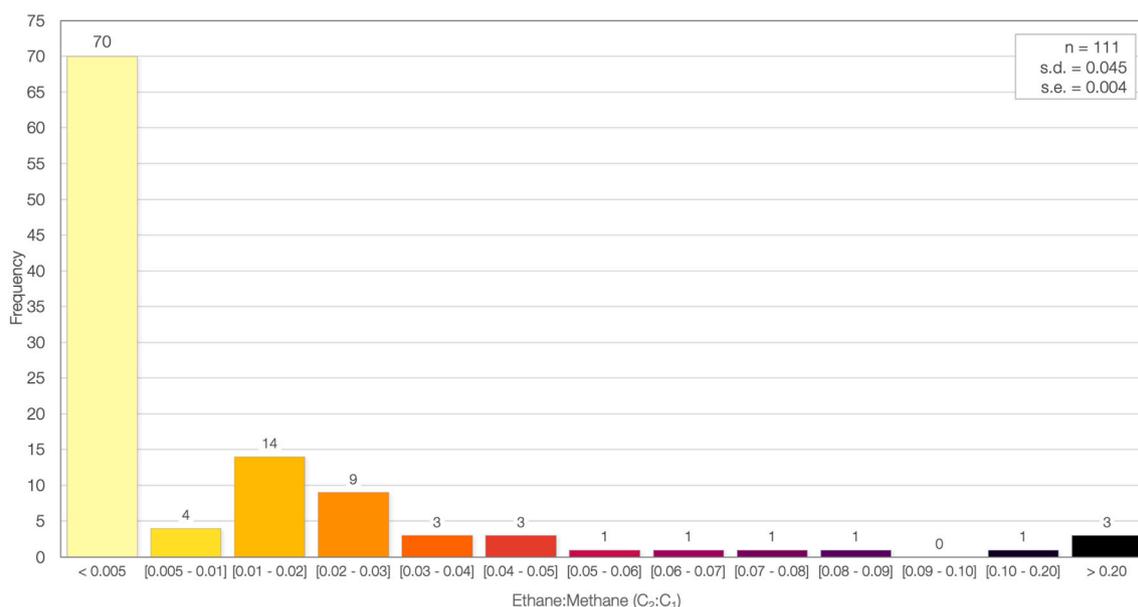

Fig. 6. Population distribution of ethane:methane ratios. Histogram showing the distribution of determined C_2:C_1 ratios from locations of enhanced CH_4 mole fractions from Bucharest, Romania. 11% of total LIs were attributed to sources using this technique. Colors correlate to ratios on Fig. 5. Biogenic sources are <0.005, thermogenic ranges from >0.005 to <0.09 and anything >0.10 is considered pyrogenic (Defratyka et al., 2021; Kort et al., 2016; Lowry et al., 2020; Yacovitch et al., 2014, 2020; Sherwood et al., 2017). (For interpretation of the references to color in this figure legend, the reader is referred to the Web version of this article.)

summer 2019 and estimated an annual emission of 140–190 tons CH_4 yr^{-1}, which is 8–10% of the annual estimates of Bucharest. The empirical method used for these studies is associated with large errors for surveys conducted in both rural and urban areas, but maybe even larger in urban environments. CH_4 enhancements can have high temporal variability, and Luetschwager et al. (2021) suggest 5–8 repeat target surveys help reduce the uncertainty of leak frequency, enhancement, and magnitude. Repeat surveys were conducted in detail for Paris and Hamburg, but were limited for the Bucharest study due to time, which may lead to an overestimation of Bucharest emissions. Measurement conditions could also pose an influence on the difference in emissions observed between cities, but all cities were measured over many days with varying wind conditions, so this should not exert as much influence as the differences in the city utility infrastructure and maintenance, where Bucharest has very different waste management protocols. Since the Hamburg and Paris studies used similar methodologies, the difference of these two cities compared to the total annual CH_4 emissions of Bucharest is probably not an artifact of the methods used. It is most likely related to differences in city leak densities and emission factors used for scaling-up.

The CH_4 LI frequency for Bucharest (Table 1) was 83%–85% larger than the leak densities used for Paris (0.11 leaks km^{-1}) and Hamburg (0.12 leaks km^{-1}). Hamburg had an emission factor that is 0.4 L min^{-1} km^{-1}, and Paris had an emission factor of 0.3 L min^{-1} km^{-1} which is only 25% and 19% of the emission factor calculated for Bucharest (1.6 L min^{-1} km^{-1}, Table 1). Downscaling the annual city-wide emissions by population, Hamburg has a CH_4 emission of 0.31 kg yr^{-1} per capita (Maazallahi et al., 2020), where in this study, the per capita emission of Bucharest is 0.83 kg yr^{-1} per capita, 63% more than Hamburg. This may indicate CH_4 emission estimations scaled by population could result in an underestimation.

Using $C_2:C_1$ ratios, $CH_4:CO_2$ ratio, and $\delta^{13}C_{CH4}$–δ^2H_{CH4}, just half (0.19 L min^{-1} km^{-1}) of the Hamburg's total emissions are from fossil fuels. Just under half of Bucharest total emission are from fossil fuels (32%–42%) resulting in a fossil fuel emission factor of 0.50–0.66 L min^{-1} km^{-1}).

5.2. Source apportionment

SI Fig. 6 shows no correlation between isotopic signature type and

flux magnitude. For a more defined source type apportionment, we look at the individual $C_2:C_1$ distribution of each emission magnitude category (Fig. 7). These skewed categorial distributions show that biogenic $C_2:C_1$ ratios dominate all emission categories, where biogenic ratios contribute to 57% of small, 61% of medium, and 77% of high emission flux rates (Table 3). Of all the calculated LI $C_2:C_1$ ratio emission estimations, 63% of the total LIs are biogenic (Table 3). Scaling our Bucharest total city-wide emission estimates (2124 L min^{-1}, Table 1) to these total source percentages, biogenic sources (wastewater) account for ~1155 ± 42 tons CH_4 yr^{-1}, thermogenic sources (natural gas) account for ~587 ± 21 tons CH_4 yr^{-1}, and pyrogenic sources contribute to ~92 ± 3 tons CH_4 yr^{-1}. Although we see that the smallest LI's add up and contribute to the majority of the total emissions (Table 3), which is similar to previously sampled cities in the U.S. (Von Fischer et al., 2017), applying the correlation between $C_2:C_1$ ratios indicates a biogenic dominance which is different from most surveyed cities. If we did not have the capability of attribution, natural gas leaks would drastically be overestimated.

Studies in other European studies, attributed more than half of the observed total city emissions to fossil fuels, Hamburg (50–80%), Utrecht (70–90%), and Paris (56%) (Maazallahi et al., 2020; Defratyka et al., 2021). Similarly, in the US, Gallagher et al., 2013 showed that emissions found in Durham, North Carolina, Manhattan, and Cincinnati, Ohio were primarily from thermogenic sources as opposed to biogenic sources. Fries et al. (2018) followed up on Gallagher's Cincinnati study (a city with an NGND pipeline replacement plan) applying source tracer measurements (N_2O, $\delta^{13}C_{CH4}$, and δ^2H_{CH4}). Of the reduced city-wide emissions, Fries et al. found that the emission sources were mostly biogenic than thermogenic, indicating that fossil fuels may have been reduced by the pipeline replacements. Both the US and European studies, as well as others, indicated that the NGDN emissions are dependent on pipeline material, age, and or maintenance practices, and demonstrate that cities with natural gas pipeline replacement plans have less leaks per distance than cities such priorities (Gallagher et al., 2015; Lamb et al., 2015; Von Fischer et al., 2017).

We assume that the dominance of wastewater emissions vs fossil fuel emissions may be a result of poor sewage infrastructure and a lack of urban city utility maintenance prioritization (Ianos et al., 2016, 2017; Kilkiş, 2016; Orlescu and Costescu, 2013; Peptenatu et al., 2012; Gogu et al., 2017). Underground sewage networks are direct sources of methane to the atmosphere (Guisasola et al., 2008; Liu et al., 2015). This
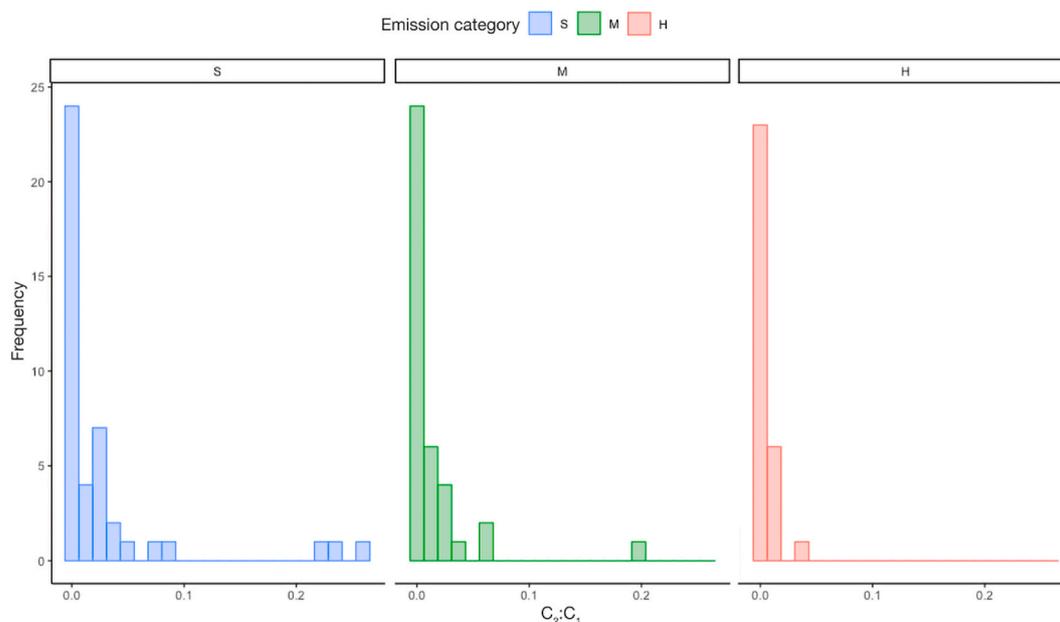

Fig. 7. Distribution of $C_2:C_1$ ratios for each emission flux category type. Histogram of $C_2:C_1$ emission flux rates (n = 111) defined by emission type, S (small) = 6 L min^{-1}, M (medium) = 6–40 L min^{-1}, H (high) = ≥ 40 L min^{-1}.

biological dominance can potentially be affected by seasonality as biogenic CH_4 produced by anaerobic digestion correlates with temperature (Lin et al., 2016), so the result only represents a snapshot of the late summer measurements. There is a lack of research focusing on CH_4 emissions from sewage network mains, especially in heavily urbanized cities like Bucharest. Therefore, more research is needed to see how much these wastewater emissions reduce during cooler and winter seasons.

5.3. Source tracer reliability

This work shows that δ^2H_{CH4} and $C_2{:}C_1$ are more valuable tracers compared to $\delta^{13}C_{CH4}$ for urban CH_4 sources in a city like Bucharest, Romania. It was difficult to assign specific source types using $\delta^{13}C_{CH4}$ due to the close similarity between signatures of background air ($\delta^{13}C_{CH4}$ -48‰ $\pm$ 1‰ s.d. (n = 14)), and ^{13}C depleted natural gas sources (50‰ $\pm$ 2 s.e. (n = 8)), with the latter overlapping with biogenic source signatures. Unlike $\delta^{13}C_{CH4}$, atmospheric background δ^2H_{CH4} (-96‰ $\pm$ 7‰ s.d.; n = 12) was relatively far from δ^2H_{CH4} signatures found for natural gas (-196‰ $\pm$ 13‰ s.e.; n = 7) and the Drumul Potcoavei leaks (-175‰ $\pm$ 2‰; n = 5). Other work also indicates that $\delta^{13}C_{CH4}$ can be an ambiguous tracer of urban CH_4 sources due to the high variability of $\delta^{13}C_{CH4}$ of natural gas which in some regions overlaps with the signatures of other sources (Townsend-Small et al., 2012, 2015, 2016; Maazallahi et al., 2020; Menoud et al., 2021). Use of $\delta^{13}C_{CH4}$ to distinguish urban sources is more successful in regions with a distinctly enriched $\delta^{13}C$ signature in the gas network, such as in UK cities (Zazzeri et al., 2015; Lowry et al., 2020) or the Netherlands (Röckmann et al., 2016; Menoud et al., 2020).

6. Conclusions

This study estimated a city emission rate of about 1832 tons CH_4 yr^{-1} (min = 1577 t yr^{-1} and max = 2113 t yr^{-1} for Bucharest and 67 tons CH_4 yr^{-1} (min = 43 t yr^{-1} and max = 110 t yr^{-1}) for Ploiesti. $C_2{:}C_1$ and δ^2H_{CH4} tracers attributed our total emissions to 58%–63% wastewater, 32%–42% natural gas, and 0–5% pyrogenic CH_4 sources (Tables 2 and 3). Measurements were made only during the summer and early autumn of 2019 and it is unknown how emissions differ during other seasons. We suspect that the large contributions of biogenic (wastewater) emission are directly related to the city sewage and wastewater infrastructure. Landfill emissions were not included in the analysis as they were outside of the city boundaries.

We found that δ^2H_{CH4} and $C_2{:}C_1$ are more useful for CH_4 source apportionment in the Bucharest area compared to $\delta^{13}C_{CH4}$. In regions of NW Europe, $\delta^{13}C_{CH4}$ is a successful source tracer (Dlugokencky et al., 2011; Maazallahi et al., 2020; Menoud et al., 2021) due to ^{13}C enriched natural gas sources of that locality, which is not the case in Bucharest. The measured CH_4 emissions in Bucharest are higher than those published in recent surveys of other European cities such as Paris (190 tons CH_4 yr^{-1}) and Hamburg (440 $\pm$ 70 tons CH_4 yr^{-1}) with large emissions both from gas leaks and wastewater. In terms of liters per minute per km, emissions from Bucharest are 4 times greater than Hamburg, Germany and 6 times greater than emissions reported from Paris, France. The proportion of emissions from sewage/wastewater was higher in Bucharest than in Hamburg and Paris. These results show the need for local governance to assess and prioritize specific city utility infrastructure maintenance.

CRediT authorship contribution statement

J.M. Fernandez: Writing – original draft, Visualization, Methodology, Validation, Isotopic, Formal analysis, Data curation, Investigation. **H. Maazallahi:** Project administration, Methodology, Software, Validation, Emission, Formal analysis, Data curation, Investigation, Writing – review & editing. **J.L. France:** Conceptualization, Methodology,

Table 2

Source tracers of locations of enhanced methane. Source categories are defined by δ^2H_{CH4} and $C_2{:}C_1$. Biogenic sources (<-270‰, <0.005) are assumed to be from wastewater and thermogenic sources ($\geq$-270‰; $\geq$0.005 to < 0.090) are assumed to be from the natural gas distribution system. $\delta^{13}C_{CH4}$ source apportionment is not utilized because observed signatures strongly overlap between biogenic (-58 to - 49‰) and thermogenic (-60 to -43‰).

Source tracer		Biogenic (wastewater)	Thermogenic (fossil fuel)	Other (Pyrogenic)
δ^2H (‰)	n	31	24	–
	Percent	58%	42%	–
$C_2{:}C_1$	n	70	37	4
	Percent	63%	32%	5%

Table 3

$C_2{:}C_1$ source type attributions by emission size category. Amount of calculated $C_2{:}C_1$ ratios that contribute to each category type. $C_2{:}C_1$ was used to define a source type for the individual emission flux rates. These rates were then assigned a category type (small, medium, high) depending on the emission rate.

Source type	stat.	Small (<6 L min^{-1})	Medium (6–40 L min^{-1})	High (>40 L min^{-1})	totals (n)	source percent
Biogenic (wastewater)	N	24	23	23	70	63%
Thermogenic (natural gas)	N	15	14	7	36	32%
Pyrogenic (combustion)	N	3	1	0	5	5%
$C_2{:}C_1$	N	42	38	30	111	100%

Software, Validation, C2:C1, Formal analysis, Data curation, Investigation, Writing – review & editing. **M. Menoud:** Methodology, Validation, Investigation, Writing – review & editing. **M. Corbu:** Project administration, Investigation. **M. Ardelean:** Project administration, Resources. **A. Calcan:** Project administration, Conceptualization, Resources. **A. Townsend-Small:** Writing – review & editing. **C. van der Veen:** Methodology, Resources. **R.E. Fisher:** Supervision, Conceptualization, Methodology, Validation, Resources, Writing – review & editing. **D. Lowry:** Supervision, Conceptualization, Methodology, Validation, Resources, Writing – review & editing. **E.G. Nisbet:** Writing – review & editing. **T. Röckmann:** Supervision, Project administration, Funding acquisition, Conceptualization, Methodology, Resources, Writing – review & editing.

Declaration of competing interest

The authors declare that they have no known competing financial interests or personal relationships that could have appeared to influence the work reported in this paper.

Acknowledgements:

Appendix A. Supplementary data

Supplementary data to this article can be found online at https://doi.org/10.1016/j.aeaoa.2022.100153.

References

Akritas, M.G., Bershady, M.A., 1996. Linear regression for astronomical data with measurement errors and intrinsic scatter. Astrophys. J. 470, 706. https://doi.org/10.1086/177901.

Alamsi, A.M., 2013. Municipal Waste Management in Romania. European Environment Agency. https://www.eea.europa.eu/publications/managing-municipal-solid-waste/romania-municipal-waste-management/view.

Amadori, M.L., Belayouni, H., Guerrera, F., Martín-Martín, M., Martin-Rojas, I., Miclăuş, C., Raffaelli, G., 2012. New data on the vrancea nappe (moldavidian basin, outer carpathian domain, Romania): paleogeographic and geodynamic reconstructions. Int. J. Earth Sci. 101, 1599–1623. https://doi.org/10.1007/s00531-011-0744-1.

Ars, S., Vogel, F., Arrowsmith, C., Heerah, S., Knuckey, E., Lavoie, J., Lee, C., Pak, N.M., Phillips, J.L., Wunch, D., 2020. Investigation of the spatial distribution of methane sources in the greater toronto area using mobile gas monitoring systems. Environ. Sci. Technol. 54, 15671–15679. https://doi.org/10.1021/acs.est.0c05386.

Bojor, J., 2010. Water and Wastewater Sectors in Romania DEMO Market Brief 2010.

BP, 2020. Statistical Review of World Energy, 68th edition, p. 66. 2020.

Brass, M., Röckmann, T., 2010. Continuous-flow isotope ratio mass spectrometry method for carbon and hydrogen isotope measurements on atmospheric methane. Atmos. Meas. Tech. 3, 1707–1721. https://doi.org/10.5194/amt-3-1707-2010.

Cambaliza, M.O.L., Shepson, P.B., Caulton, D.R., Stirm, B., Samarov, D., Gurney, K.R., Turnbull, J., Davis, K.J., Possolo, A., Karion, A., Sweeney, C., Moser, B., Hendricks, A., Lauvaux, T., Mays, K., Whetstone, J., Huang, J., Razlivanov, I., Miles, N.L., Richardson, S.J., 2014. Assessment of uncertainties of an aircraft-based mass balance approach for quantifying urban greenhouse gas emissions. Atmos. Chem. Phys. 14, 9029–9050. https://doi.org/10.5194/acp-14-9029-2014.

Chamberlain, S.D., Ingraffea, A.R., Sparks, J.P., 2016. Sourcing methane and carbon dioxide emissions from a small city: influence of natural gas leakage and combustion. Environ. Pollut. 218, 102–110. https://doi.org/10.1016/j.envpol.2016.08.036.

Clayton, C., 1991. Carbon isotope fractionation during natural gas generation from kerogen. Mar. Petrol. Geol. 8, 232–240. https://doi.org/10.1016/0264-8172(91)90010-X.

Coleman, D.D., Risatti, J.B., Schoell, M., 1981. Fractionation of carbon and hydrogen isotopes by methane-oxidizing bacteria. Geochem. Cosmochim. Acta 45, 1033–1037. https://doi.org/10.1016/0016-7037(81)90129-0.

Cranganu, C., Deming, D., 1996. Heat flow and hydrocarbon generation in the Transylvanian Basin, Romania. Am. Assoc. Petrol. Geol. Bull. 80, 1641–1653. https://doi.org/10.1306/64eda0e6-1724-11d7-8645000102c1865d.

Deaconu, S., 2020. Romania's Greenhouse Gas Inventory 1989-2018, National Inventory Report. Ministry of Environment, Waters and Forests National Environmental Protection Agency, Romania.

Defratyka, S.M., Paris, J.D., Yver-Kwok, C., Fernandez, J.M., Korben, P., Bousquet, P., 2021. Mapping urban methane sources in Paris, France. Environ. Sci. Technol. https://doi.org/10.1021/acs.est.1c00859.

Dlugokencky, E.J., Nisbet, E.G., Fisher, R., Lowry, D., 2011. Global atmospheric methane: budget, changes and dangers. Philos. Trans. R. Soc. A Math. Phys. Eng. Sci. https://doi.org/10.1098/rsta.2010.0341.

Fisher, R., Lowry, D., Wilkin, O., Sriskantharajah, S., Nisbet, E.G., 2006. High-precision, automated stable isotope analysis of atmospheric methane and carbon dioxide using continuous-flow isotope-ratio mass spectrometry. Rapid Commun. Mass Spectrom. 20, 200–208. https://doi.org/10.1002/rcm.2300.

France, J.L., Cain, M., Fisher, R.E., Lowry, D., Allen, G., O'Shea, S.J., Illingworth, S., Pyle, J., Warwick, N., Jones, B.T., Gallagher, M.W., Bower, K., Le Breton, M., Percival, C., Muller, J., Welpott, A., Bauguitte, S., George, C., Hayman, G.D., Manning, A.J., Lund Myhre, C., Lanoisellé, M., Nisbet, E.G., 2016. Measurements of δ13C in CH4 and using particle dispersion modeling to characterize sources of arctic methane within an air mass. J. Geophys. Res. 121, 257–270. https://doi.org/10.1002/2016JD026006.

Fries, A.E., Schifman, L.A., Shuster, W.D., Townsend-Small, A., 2018. Street-level emissions of methane and nitrous oxide from the wastewater collection system in Cincinnati, Ohio. Environ. Pollut. 236, 247–256. https://doi.org/10.1016/j.envpol.2018.01.076.

Gallagher, M.E., Down, A., Ackley, R.C., Zhao, K., Phillips, N., Jackson, R.B., 2015. Natural gas pipeline replacement programs reduce methane leaks and improve consumer safety. Environ. Sci. Technol. Lett. 2, 286–291. https://doi.org/10.1021/acs.estlett.5b00213.

Gioli, B., Toscano, P., Lugato, E., Matese, A., Miglietta, F., Zaldei, A., Vaccari, F.P., 2012. Methane and carbon dioxide fluxes and source partitioning in urban areas: the case study of Florence, Italy. Environ. Pollut. 164, 125–131. https://doi.org/10.1016/j.envpol.2012.01.019.

Gogu, C.R., Gaitanaru, D., Boukhemacha, M.A., Serpescu, I., Litescu, L., Zaharia, V., Moldovan, A., Mihailovici, M.J., 2017. Urban hydrogeology studies in bucharest city, Romania. Procedia Eng. 209, 135–142. https://doi.org/10.1016/j.proeng.2017.11.139.

Guisasola, A., de Haas, D., Kelle, J., Yuan, Z., 2008. Methane formation in sewer systems. Water Res. 42, 1421–1430. https://doi.org/10.1016/j.watres.2007.10.014.

Han, Z.Y., Weng, W.G., 2010. An integrated quantitative risk analysis method for natural gas pipeline network. J. Loss Prev. Process. Ind. 23, 428–436. https://doi.org/10.1016/j.jlp.2010.02.003.

Harrison, M.R., Shires, T.M., Wessels, J.K., Cowgill, R.M., 1996. Methane Emissions from the Natural Gas Industry, , Final Report1-15. Gas Research Institute/Environmental Protection Agency, Washington, DC. https://www.epa.gov/sites/default/files/2016-08/documents/1_executiveummary.pdf.

Helfter, C., Tremper, A.H., Halios, C.H., Kotthaus, S., Bjorkegren, A., Grimmond, C.S.B., Barlow, J.F., Nemitz, E., 2016. Spatial and temporal variability of urban fluxes of methane, carbon monoxide and carbon dioxide above London, UK. Atmos. Chem. Phys. 16, 10543–10557. https://doi.org/10.5194/acp-16-10543-2016.

Hendrick, M.F., Ackley, R., Sanaie-Movahed, B., Tang, X., Phillips, N.G., 2016. Fugitive methane emissions from leak-prone natural gas distribution infrastructure in urban environments. Environ. Pollut. 213, 710–716. https://doi.org/10.1016/j.envpol.2016.01.094.

Iacoboaea, C., Petrescu, F., 2013. Landfill monitoring using remote sensing: a case study of Glina, Romania. Waste Manag. Res. 31, 1075–1080. https://doi.org/10.1177/0734242X13487585.

Ianoş, I., Zamfir, D., Stoica, V., Cercleux, L., Schvab, A., Pascariu, G., 2012. Municipal solid waste management for sustainable development of Bucharest metropolitan area. Environ. Eng. Manag. J. 11, 359–369. https://doi.org/10.30638/eemj.2012.045.

Ianoş, I., Sorensen, A., Merciu, C., 2016. Incoherence of urban planning policy in Bucharest: its potential for land use conflict. Land Use Pol. 60, 101–112. https://doi.org/10.1016/j.landusepol.2016.10.030.

IPCC, 2014. Climate change 2014: mitigation of climate change. In: Edenhofer, O., Pichs-Madruga, R., Sokona, Y., Farahani, E., Kadner, S., Seyboth, K., Adler, A., Baum, I., Brunner, S., Eickemeier, P., Kriemann, B., Savolainen, J., Schlömer, S., von Stechow, C., Zwickel, T., Minx, J.C. (Eds.), Contribution of Working Group III to the Fifth Assessment Report of the Intergovernmental Panel on Climate Change. Cambridge University Press.

Jackson, S.M., Morgan, G.H., Morse, A.D., Butterworth, A.L., Pillinger, C.T., 1999. The use of static mass spectrometry to determine the combined stable isotopic composition of small samples of atmospheric methane. Rapid Commun. Mass Spectrom. 13, 1329–1333. https://doi.org/10.1002/(SICI)1097-0231(19990715)13:13<1329::AID-RCM648>3.0.CO;2-P.

Jackson, R.B., Down, A., Phillips, N.G., Ackley, R.C., Cook, C.W., Plata, D.L., Zhao, K., 2014. Natural gas pipeline leaks across Washington, DC. Environ. Sci. Technol. 48, 2051–2058. https://doi.org/10.1021/es404474x.

James, A.T., 1983. Correlation of natural gas by use of carbon isotopic distribution between hydrocarbon components. Am. Assoc. Petrol. Geol. Bull. 67, 1176–1191. https://doi.org/10.1306/03B5B722-16D1-11D7-8645000102C1865D.

Keeling, C.D., 1958. The concentration and isotopic abundances of atmospheric carbon dioxide in rural areas. Geochem. Cosmochim. Acta 13, 322–334. https://doi.org/10.1016/0016-7037(58)90033-4.

Keeling, C.D., 1961. The concentration and isotopic abundances of carbon dioxide in rural and marine air. Geochem. Cosmochim. Acta 13, 322–334. https://doi.org/10.1016/0016-7037(58)90033-4.

Kilkis, S., 2016. Sustainable development of energy, water and environment systems index for Southeast European cities. J. Clean. Prod. 130, 222–234. https://doi.org/10.1016/j.jclepro.2015.07.121.

Kirschke, S., Bousquet, P., Ciais, P., Saunois, M., Canadell, J.G., Dlugokencky, E.J., Bergamaschi, P., Bergmann, D., Blake, D.R., Bruhwiler, L., Cameron-Smith, P., Castaldi, S., Chevallier, F., Feng, L., Fraser, A., Heimann, M., Hodson, E.L., Houweling, S., Josse, B., Fraser, P.J., Krummel, P.B., Lamarque, J.F., Langenfelds, R. L., Le Quéré, C., Naik, V., O'doherty, S., Palmer, P.I., Pison, I., Plummer, D., Poulter, B., Prinn, R.G., Rigby, M., Ringeval, B., Santini, M., Schmidt, M., Shindell, D. T., Simpson, I.J., Spahni, R., Steele, L.P., Strode, S.A., Sudo, K., Szopa, S., Van Der Werf, G.R., Voulgarakis, A., Van Weele, M., Weiss, R.F., Williams, J.E., Zeng, G., 2013. Three decades of global methane sources and sinks. Nat. Geosci. https://doi.org/10.1038/ngeo1955.

Kuc, T., Rozanski, K., Zimnoch, M., Necki, J., Korus, A., 2003. Anthropogenic emissions of CO2 and CH4 in an urban environment. Appl. Energy 75, 193–203. https://doi.org/10.1016/S0306-2619(03)00032-1.

Lamb, B.K., Edburg, S.L., Ferrara, T.W., Howard, T., Harrison, M.R., Kolb, C.E., Townsend-Small, A., Dyck, W., Possolo, A., Whetstone, J.R., 2015. Direct measurements show decreasing methane emissions from natural gas local distribution systems in the United States. Environ. Sci. Technol. 49, 5161–5169. https://doi.org/10.1021/es505116p.

Lamb, B.K., Cambaliza, M.O.L., Davis, K.J., Edburg, S.L., Ferrara, T.W., Floerchinger, C., Heimburger, A.M.F., Herndon, S., Lauvaux, T., Lavoie, T., Lyon, D.R., Miles, N., Prasad, K.R., Richardson, S., Roscioli, J.R., Salmon, O.E., Shepson, P.B., Stirm, B.H., Whetstone, J., 2016. Direct and indirect measurements and modeling of methane emissions in Indianapolis, Indiana. Environ. Sci. Technol. 50, 8910–8917. https://doi.org/10.1021/acs.est.6b01198.

Lin, Q., Vrieze, J.D., He, G., Li, X., Li, J., 2016. Temperature regulates methane production through the function centralization of microbial community in anaerobic digestion. Bioresourc. Tech. 216, 150–158. https://doi.org/10.1016/j.biortech.2016.05.046.

Liu, Y., Ni, B.J., Sharma, K.R., Yuan, Z., 2015. Methane emission from sewers. Sci. Total Environ. 524, 40–51. https://doi.org/10.1016/j.scitotenv.2015.04.029.

Lowry, D., Holmes, C.W., Rata, N.D., O'Brien, P., Nisbet, E.G., 2001. London methane emissions: use of diurnal changes in concentration and δ 13 C to identify urban sources and verify inventories. J. Geophys. Res. Atmos. 106, 7427–7448. https://doi.org/10.1029/2000JD900601.

Lowry, D., Fisher, R.E., France, J.L., Coleman, M., Lanoisellé, M., Zazzeri, G., Nisbet, E. G., Shaw, J.T., Allen, G., Pitt, J., Ward, R.S., 2020. Environmental baseline monitoring for shale gas development in the UK: identification and geochemical characterisation of local source emissions of methane to atmosphere. Sci. Total Environ. 708, 134600 https://doi.org/10.1016/j.scitotenv.2019.134600.

Luetschwager, E., von Fischer, J.C., Weller, Z.D., 2021. Characterizing detection probabilities of advanced mobile leak surveys: implications for sampling effort and leak size estimation in natural gas distribution systems. Elem. Sci. Anth. 9, 1. https://doi.org/10.1525/elementa.2020.00143.

Ma, L., Cheng, L., Li, M., 2013. Quantitative risk analysis of urban natural gas pipeline networks using geographical information systems. J. Loss Prev. Process. Ind. 26, 1183–1192. https://doi.org/10.1016/j.jlp.2013.05.001.

Maazallahi, H., Fernandez, J.M., Menoud, M., Zavala-araiza, D., Weller, Z.D., Schwietzke, S., Gon, H.D. Van Der, 2020. Methane mapping , emission quantification and attribution in two European cities ; Utrecht , NL and Hamburg , DE 1–30. Atmos. Chem. Phys. 20, 14717–14740. https://doi.org/10.5194/acp-20-14717-2020, 2020.

Mays, K.L., Shepson, P.B., Stirm, B.H., Karion, A., Sweeney, C., Gurney, K.R., 2009. Aircraft-based measurements of the carbon footprint of Indianapolis. Environ. Sci. Technol. 43, 7816–7823. https://doi.org/10.1021/es901326b.

McKain, K., Down, A., Raciti, S.M., Budney, J., Hutyra, L.R., Floerchinger, C., Herndon, S.C., Nehrkorn, T., Zahniser, M.S., Jackson, R.B., Phillips, N., Wofsy, S.C., 2015. Methane emissions from natural gas infrastructure and use in the urban region of Boston, Massachusetts. Proc. Natl. Acad. Sci. Unit. States Am. 112, 1941–1946. https://doi.org/10.1073/pnas.1416261112.

Menoud, M., van der Veen, C., Scheeren, B., Chen, H., Szénási, B., Morales, R.P., Pison, I., Bousquet, P., Brunner, D., Röckmann, T., 2020. Characterisation of methane sources in Lutjewad, The Netherlands, using quasi-continuous isotopic composition measurements. Tellus B. https://doi.org/10.1080/16000889.2020.1823733.

Menoud, Malika, van der Veen, Carina, Necki, Jaroslaw, Bartyzel, Jakub, Szenasi, Barbara, Stanisavljevic, Mila, Pison, Isabelle, Bousquet, Philippe, Röckmann, Thomas, 2021. Methane (CH_4) sources in Krakow, Poland: insights from isotope analysis, 10.5194/acp-2021-146 Chem. Phys. Discuss.. https://doi.org/10.5194/acp-2021-146 [preprint].

Miller, S.M., Wofsy, S.C., Michalak, A.M., Kort, E.A., Andrews, A.E., Biraud, S.C., Dlugokencky, E.J., Eluszkiewicz, J., Fischer, M.L., Janssens-Maenhout, G., Miller, B. R., Miller, J.B., Montzka, S.A., Nehrkorn, T., Sweeney, C., 2013. Anthropogenic emissions of methane in the United States. Proc. Natl. Acad. Sci. U.S.A. 110, 20018–20022. https://doi.org/10.1073/pnas.1314392110.

Mischler, J.A., Sowers, T.A., Alley, R.B., Battle, M., McConnell, J.R., Mitchell, L., Popp, T., Sofen, E., Spencer, M.K., 2009. Carbon and hydrogen isotopic composition of methane over the last 1000 years. Global Biogeochem. Cycles 23. https://doi.org/10.1029/2009GB003460 n/a-n/a.

Myhre, G., Shindell, D., Bréon, F.-M., Collins, W., Fuglestvedt, J., Huang, J., Koch, D., Lamarque, J.-F., Lee, D., Mendoza, B., Nakajima, T., Robock, A., Stephens, G., Takemura, T., Zhang, H., 2013. Anthropogenic and natural radiative forcing. In: Stocker, T.F., Qin, D., Plattner, D., K, G., Tignor, M., Allen, S.K., Boschung, J., Nauels, A., Xia, Y., Bex, V., Midgley, P.M. (Eds.), Climate Change 2013: The Physical Science Basis. Contribution of Working Group I to the Fifth Assessment Report of the Intergovernmental Panel on Climate Change. Cambridge University Press, Cambridge, United Kingdom and New York, NY, USA.

Nae, M., Turnock, D., 2011. The new Bucharest: Two decades of restructuring. Cities 28 (2), 206–219. https://doi.org/10.1016/j.cities.2010.04.004.

Romania National Institute for Statistics (NIS), 2020. TEMPO-online. ©The national Institute of statistics Romania 1998 – 2018. Contains public information based on open government license v1.0. http://statistici.insse.ro:8077/tempoonline/#/pages/tables/insse-table.

Nisbet, E.G., Manning, M.R., Dlugokencky, E.J., Fisher, R.E., Lowry, D., Michel, S.E., Lund Myhre, C., Platt, S.M., Allen, G., Bousquet, P., Brownlow, R., Cain, M., France, J.L., Hermannsen, O., Hossaini, R., Jones, A.E., Levin, I., Manning, A.C., Myhre, G., Pyle, J.A., Vaughn, B.H., Warwick, N.J., White, J.W., 2019. Very strong atmospheric methane growth in the 4 Years 2014 – 2017 : implications for the Paris agreement. Global Biogeochem. Cycles 318–342. https://doi.org/10.1029/2018GB006009.

Nisbet, E.G., Fisher, R.E., Lowry, D., France, J.L., Allen, G., Bakkaloglu, S., Broderick, T. J., Cain, M., Coleman, M., Fernandez, J., Forster, G., Griffiths, P.T., Iverach, C.P., Kelly, B.F.J., Manning, M.R., Nisbet-Jones, P.B.R., Pyle, J.A., Townsend-Small, A., Al-Shalaan, A., Warwick, N., Zazzeri, G., 2020. Methane mitigation: methods to reduce emissions, on the Path to the Paris agreement. Rev. Geophys. 58, 1–51. https://doi.org/10.1029/2019RG000675.

Nita, R., 2018. World's First Oil Refinery: the City of Ploieşti. World Recor Acad. LLC, pp. 1–7.

O'Shea, S.J., Allen, G., Fleming, Z.L., Bauguitte, S.J.B., Percival, C.J., Gallagher, M.W., Lee, J., Helfter, C., Nemitz, E., 2014. Area fluxes of carbon dioxide, methane, and carbon monoxide derived from airborne measurements around Greater London: a case study during summer 2012. J. Geophys. Res. Atmos. 119, 4940–4952. https://doi.org/10.1002/2013JD021269.

Pataki, D.E., Bowling, D.R., Ehleringer, J.R., 2003. Seasonal cycle of carbon dioxide and its isotopic composition in an urban atmosphere: Anthropogenic and biogenic effects. J. Geophys. Res. 108, 4735. https://doi.org/10.1029/2003JD003865. https://doi.org/10.1029/2003JD003865.

Peischl, J., Ryerson, T.B., Brioude, J., Aikin, K.C., Andrews, A.E., Atlas, E., Blake, D., Daube, B.C., De Gouw, J.A., Dlugokencky, E., Frost, G.J., Gentner, D.R., Gilman, J.B., Goldstein, A.H., Harley, R.A., Holloway, J.S., Kofler, J., Kuster, W.C., Lang, P.M., Novelli, P.C., Santoni, G.W., Trainer, M., Wofsy, S.C., Parrish, D.D., 2013. Quantifying sources of methane using light alkanes in the Los Angeles basin,

California. J. Geophys. Res. Atmos. 118, 4974–4990. https://doi.org/10.1002/jgrd.50413.

Peptenatu, D., Pintilii, R.D., Draghici, C., Merciu, C., Mateescu, R.D., 2012. Management of environment risk within emergency territorial systems. case study the influence area of the bucharest city. J. Environ. Prot. Ecol. 13, 2360–2370.

Phillips, N.G., Ackley, R., Crosson, E.R., Down, A., Hutyra, L.R., Brondfield, M., Karr, J. D., Zhao, K., Jackson, R.B., 2013. Mapping urban pipeline leaks: methane leaks across Boston. Environ. Pollut. 173, 1–4. https://doi.org/10.1016/j.envpol.2012.11.003.

Picarro, 2017a. G2401 Analyzer Datasheet. V1.0, 1–2. Santa Clara, CA.

Picarro, 2017b. GasScouterTM G4302 Analyzer Datasheet. V1.0,1–2. Santa Clara, CA.

Picarro, 2019. G2301 Analyzer Datasheet. V1.1, 1–2. Santa Clara, CA.

Röckmann, T., Eyer, S., van der Veen, C., Popa, M.E., Tuzson, B., Monteil, G., Houweling, S., Harris, E., Brunner, D., Fischer, H., Zazzeri, G., Lowry, D., Nisbet, E. G., Brand, W.A., Necki, J.M., Emmenegger, L., Mohn, J., 2016. In situ observations of the isotopic composition of methane at the Cabauw tall tower site. Atmos. Chem. Phys. 16, 10469–10487. https://doi.org/10.5194/acp-16-10469-2016.

Sandulescu, E., 2004. The contribution of waste management to the reduction of greenhouse gas emissions with applications in the city of Bucharest. Waste Manag. Res. 22, 413–426. https://doi.org/10.1177/0734242X04048519.

Saunois, M., Stavert, A.R., Poulter, B., Bousquet, P., Canadell, J.G., Jackson, R.B., Raymond, P.A., Dlugokencky, E.J., Houweling, S., Patra, P.K., Ciais, P., Arora, V.K., Bastviken, D., Bergamaschi, P., Blake, D.R., Brailsford, G., Bruhwiler, L., Carlson, K. M., Carrol, M., Castaldi, S., Chandra, N., Crevoisier, C., Crill, P.M., Covey, K., Curry, C.L., Etiope, G., Frankenberg, C., Gedney, N., Hegglin, M.I., Höglund-Isakson, L., Hugelius, G., Ishizawa, M., Ito, A., Janssens-Maenhout, G., Jensen, K.M., Joos, F., Kleinen, T., Krummel, P.B., Langenfelds, R.L., Laruelle, G.G., Liu, L., Machida, T., Maksyutov, S., McDonald, K.C., McNorton, J., Miller, P.A., Melton, J.R., Morino, I., Müller, J., Murgia-Flores, F., Naik, V., Niwa, Y., Noce, S., O& apos, Doherty, S., Parker, R.J., Peng, C., Peng, S., Peters, G.P., Prigent, C., Prinn, R., Ramonet, M., Regnier, P., Riley, W.J., Rosentreter, J.A., Segers, A., Simpson, I.J., Shi, H., Smith, S.J., Steele, L.P., Thornton, B.F., Tian, H., Tohjima, Y., Tubiello, F.N., Tsuruta, A., Viovy, N., Voulgarakis, A., Weber, T.S., van Weele, M., van der Werf, G. R., Weiss, R.F., Worthy, D., Wunch, D., Yin, Y., Yoshida, Y., Zhang, W., Zhang, Z., Zhao, Y., Zheng, B., Zhu, Qing, Zhu, Qiuan, Zhuang, Q., 2020. The global methane budget 2000-2017. Earth Syst. Sci. Data Discuss. 1–138. https://doi.org/10.5194/essd-2019-128.

Scarpelli, T.R., Jacob, D.J., Maasakkers, J.D., Sulprizio, M.P., Sheng, J.X., Rose, K., Romeo, L., Worden, J.R., Janssens-Maenhout, G., 2020. A global gridded ($0.1°$ × $0.1°$) inventory of methane emissions from oil, gas, and coal exploitation based on national reports to the United Nations Framework Convention on Climate Change. Earth Syst. Sci. Data 12, 563–575. https://doi.org/10.5194/essd-12-563-2020.

Schoell, M., 1984. Recent advances in petroleum isotope geochemistry. Org. Geochem. 6, 645–663. https://doi.org/10.1016/0146-6380(84)90086-X.

Schoell, M., 1988. Multiple origins of methane in the Earth. Chem. Geol. 71, 1–10. https://doi.org/10.1016/0009-2541(88)90101-5.

Sclater, J., Royden, L., Horath, F., Burchfield, B., Semken, S., Stegena, L., 1980. The formation of the intra-carpathian basins as determined from subsidence data. Earth Planet Sci. Lett. 51, 139–162. https://doi.org/10.1016/0012-821X(80)90262-9.

Sherwood, O.A., Schwietzke, S., Arling, V.A., Etiope, G., 2017. Global inventory of gas geochemistry data from fossil fuel, microbial and burning sources, version 2017. Earth Syst. Sci. Data 9, 639–656. https://doi.org/10.5194/essd-9-639-2017.

Sowers, T., 2010. Atmospheric methane isotope records covering the Holocene period. Quat. Sci. Rev. 29, 213–221. https://doi.org/10.1016/j.quascirev.2009.05.023.

Sperlich, P., Uitslag, N.A.M., Richter, J.M., Rothe, M., Geilmann, H., Veen, C. Van Der, Röckmann, T., Blunier, T., Brand, W.A., 2016. Development and evaluation of a suite of isotope reference gases for methane in air. Atmos. Meas. Tech. 9, 3717–3737. https://doi.org/10.5194/amt-9-3717-2016.

Townsend-Small, A., Tyler, S.C., Pataki, D.E., Xu, X., Christensen, L.E., 2012. Isotopic measurements of atmospheric methane in Los Angeles, California, USA: influence of "fugitive" fossil fuel emissions. J. Geophys. Res. Atmos. (117) https://doi.org/10.1029/2011JD016826.

Townsend-Small, A., Marrero, J.E., Lyon, D.R., Simpson, I.J., Meinardi, S., Blake, D.R., 2015. Integrating source apportionment tracers into a bottom-up inventory of methane emissions in the Barnett shale hydraulic fracturing region. Environ. Sci. Technol. 49, 8175–8182. https://doi.org/10.1021/acs.est.5b00057.

Townsend-Small, A., Botner, E.C., Jimenez, K.L., Schroeder, J.R., Blake, N.J., Meinardi, S., Blake, D.R., Sive, B.C., Bon, D., Crawford, J.H., Pfister, G., Flocke, F.M., 2016. Using stable isotopes of hydrogen to quantify biogenic and thermogenic atmospheric methane sources: a case study from the Colorado Front Range. Geophys. Res. Lett. 43, 462–471. https://doi.org/10.1002/2016GL071438.

UNFCCC, 2019. Romania's Fourth Biennial Report, December 2019. Ministry of Environment, Waters & Forest, Romania.

U.S. EPA, 2020. Greenhouse gas Equivalencies calculator. https://www.epa.gov/energy/greenhouse-gas-equivalencies-calculator. Accessed 2021/02/05.

Veolia, K., 2013. Glina Wastewater Treatment Plant , Romania Bioflex – Increased Biological Capacity. Case Study.

Von Fischer, J.C., Cooley, D., Chamberlain, S., Gaylord, A., Griebenow, C.J., Hamburg, S. P., Salo, J., Schumacher, R., Theobald, D., Ham, J., 2017. Rapid, vehicle-based identification of location and magnitude of urban natural gas pipeline leaks. Environ. Sci. Technol. 51, 4091–4099. https://doi.org/10.1021/acs.est.6b06095.

Weller, Z.D., Roscioli, J.R., Daube, W.C., Lamb, B.K., Ferrara, T.W., Brewer, P.E., von Fischer, J.C., 2018. Vehicle-based methane surveys for finding natural gas leaks and estimating their size: validation and uncertainty. Environ. Sci. Technol. 52 https://doi.org/10.1021/acs.est.8b03135 acs.est.8b03135.

Weller, Z.D., Yang, D.K., von Fischer, J.C., 2019. An open source algorithm to detect natural gas leaks from mobile methane survey data. PLoS One 14, e0212287. https://doi.org/10.1371/journal.pone.0212287.

Wennberg, P.O., Mui, W., Wunch, D., Kort, E.A., Blake, D.R., Atlas, E.L., Santoni, G.W., Wofsy, S.C., Diskin, G.S., Jeong, S., Fischer, M.L., 2012. On the sources of methane to the Los Angeles atmosphere. Environ. Sci. Technol. 46, 9282–9289. https://doi.org/10.1021/es301138y.

Whiticar, M.J., 1990. A geochemical perspective of natural gas and atmospheric methane. Org. Geochem. 16, 531–547. https://doi.org/10.1016/0146-6380(90)90068-B.

WMO, 2020. The state of greenhouse gases in the atmosphere based on global observations through 2019. WMO Greenh. Gas Bull. 16, 1–9. https://gaw.kishou.go.jp/static/publications/bulletin/Bulletin2019/ghg-bulletin-16.pdf.

Worden, J.R., Bloom, A.A., Pandey, S., Jiang, Z., Worden, H.M., Walker, T.W., Houweling, S., Röckmann, T., 2017. Reduced biomass burning emissions reconcile conflicting estimates of the post-2006 atmospheric methane budget. Nat. Commun. 8 https://doi.org/10.1038/s41467-41017-02246-41460. ARTN 2227.

Wunch, D., Toon, G.C., Hedelius, J.K., Vizenor, N., Roehl, C.M., Saad, K.M., Blavier, J.-F. L., Blake, D.R., Wennberg, P.O., 2016. Quantifying the loss of processed natural gas within California's South Coast Air Basin using long-term measurements of ethane and methane. Atmos. Chem. Phys. 16, 14091–14105. https://doi.org/10.5194/acp-16-14091-2016.

Xueref-Remy, I., Zazzeri, G., Bréon, F.M., Vogel, F., Ciais, P., Lowry, D., Nisbet, E.G., 2020. Anthropogenic methane plume detection from point sources in the Paris megacity area and characterization of their δ13C signature. Atmos. Environ. 222 https://doi.org/10.1016/j.atmosenv.2019.117055.

Yacovitch, T.I., Herndon, S.C., Roscioli, J.R., Floerchinger, C., McGovern, R.M., Agnese, M., Pétron, G., Kofler, J., Sweeney, C., Karion, A., Conley, S.A., Kort, E.A., Nähle, L., Fischer, M., Hildebrandt, L., Koeth, J., McManus, J.B., Nelson, D.D., Zahniser, M.S., Kolb, C.E., 2014. Demonstration of an ethane spectrometer for methane source identification. Environ. Sci. Technol. 48, 8028–8034. https://doi.org/10.1021/es501475q.

Yarnes, C., 2013. δ 13 C and δ 2 H measurement of methane from ecological and geological sources by gas chromatography/combustion/pyrolysis isotope-ratio mass spectrometry. Rapid Commun. Mass Spectrom. 27, 1036–1044. https://doi.org/10.1002/rcm.6549.

Zazzeri, G., 2015. Methane Emissions in UK: Deciphering Regional Sources with Mobile Measurements and Isotopic Characterisation. Royal Holloway, University of London.

Zazzeri, G., Lowry, D., Fisher, R., France, J.L., Lanoisellé, M., Nisbet, E.G., 2015. Plume mapping and isotopic characterisation of anthropogenic methane sources. Atmos. Environ. 110, 151–162. https://doi.org/10.1016/j.atmosenv.2015.03.029.

Zazzeri, G., Lowry, D., Fisher, R.E., France, J.L., Lanoisellé, M., Kelly, B.F.J., Necki, J.M., Iverach, C.P., Ginty, E., Zimnoch, M., Jasek, A., Nisbet, E.G., 2016. Carbon isotopic signature of coal-derived methane emissions to the atmosphere: from coalification to alteration. Atmos. Chem. Phys. 16, 13669–13680. https://doi.org/10.5194/acp-16-13669-2016.

Zazzeri, G., Lowry, D., Fisher, R.E., France, J.L., Lanoisellé, M., Grimmond, C.S.B., Nisbet, E.G., 2017. Evaluating methane inventories by isotopic analysis in the London region. Sci. Rep. 7, 4854. https://doi.org/10.1038/s41598-017-04802-6.

Zimnoch, M., Godlowska, J., Necki, J.M., Rozanski, K., 2010. Assessing surface fluxes of CO 2 and CH 4 in urban environment: a reconnaissance study in Krakow, Southern Poland. Tellus B Chem. Phys. Meteorol. 62, 573–580. https://doi.org/10.1111/j.1600-0889.2010.00489.

Zimnoch, M., Necki, J., Chmura, L., Jasek, A., Jelen, D., Galkowski, M., Kuc, T., Gorczyca, Z., Bartyzel, J., Rozanski, K., 2018. Quantification of carbon dioxide and methane emissions in urban areas: source apportionment based on atmospheric observations. Mitig. Adapt. Strategies Glob. Change 24, 1051–1071. https://doi.org/10.1007/s11027-018-9821-0.

Zolin, M.B., 2007. The extended metropolitan area in a new EU member state: implications for a rural development approach. Transit. Stud. Rev. 14, 565–573. https://doi.org/10.1007/s11300-007-0154-z.